



Article

Precipitation and Temperature Trends and Cycles Derived from Historical 1890–2019 Weather Data for the City of Ottawa, Ontario, Canada

Carling Ruth Walsh * and R. Timothy Patterson

Ottawa Carleton Geoscience Center and Department of Earth Sciences, Carleton University, Ottawa, ON K1S 5B6, Canada; timpatterson@cunet.carleton.ca

* Correspondence: carling.walsh@carleton.ca

Abstract: Patterns in historical climate data were analyzed for Ottawa, Ontario, Canada, for the interval 1890–2019. Variables analyzed included records of annual, seasonal, and extreme temperature and precipitation, diurnal temperature range, and various environmental responses. Using LOWESS regressions, it was found that annual and seasonal temperatures in Ottawa have generally increased through this interval, precipitation has shifted to a less snowy, rainier regime, and diurnal temperature variation has decreased. Furthermore, the annual growing season has lengthened by 23 days to ~163 days, and the annual number of frost-free days increased by 13 days to ~215 days. Despite these substantial climatic shifts, some variables (e.g., extreme weather events per year) have remained largely stable through the interval. Time-series analyses (including multitaper spectral analysis and continuous and cross wavelet transforms) have revealed the presence of several strong cyclical patterns in the instrumental record attributable to known natural climate phenomena. The strongest such influence on Ottawa’s climate has been the 11-year solar cycle, while the influence of the El Niño–Southern Oscillation, Arctic Oscillation, North Atlantic Oscillation, and Quasi-Biennial Oscillation were also observed and linked with the trends in annual, seasonal, and extreme weather. The results of this study, particularly the observed linkages between temperature and precipitation variables and cyclic climate drivers, will be of considerable use to policymakers for the planning, development, and maintenance of city infrastructure as Ottawa continues to rapidly grow under a warmer, wetter climate regime.

Keywords: climate change; climate teleconnections; time series analysis; historical temperature precipitation



Citation: Walsh, C.R.; Patterson, R.T. Precipitation and Temperature Trends and Cycles Derived from Historical 1890–2019 Weather Data for the City of Ottawa, Ontario, Canada. *Environments* **2022**, *9*, 35. <https://doi.org/10.3390/environments9030035>

Academic Editors: Hsiao-Chi Chuang, Yongming Han, Didik Setyo Heriyanto and Kin-Fai Ho

Received: 28 January 2022

Accepted: 4 March 2022

Published: 9 March 2022

Publisher’s Note: MDPI stays neutral with regard to jurisdictional claims in published maps and institutional affiliations.



Copyright: © 2022 by the authors. Licensee MDPI, Basel, Switzerland. This article is an open access article distributed under the terms and conditions of the Creative Commons Attribution (CC BY) license (<https://creativecommons.org/licenses/by/4.0/>).

1. Introduction

Since the late 1980s, the potential environmental impact of a warming world has become an increasingly prominent focus of political discourse (e.g., [1–3]). The analysis of global or regional trends dominates both the scientific and popular literature. For example, in North America, there is a large body of scientific literature assessing climate trends at not only the continental scale but also at the regional level, as well as at the provincial and state level [4–11]. However, there is a dearth of analysis of more localized climate trends. Such data is highly useful, though, as local climate variations can differ significantly, either periodically or as part of longer-term temporal trends, from regional or global records [12,13]. By studying existing localized historical temperature and precipitation records, an objective assessment of the nature of fine-scale climate trends can be made, which in turn can be used to make a more realistic assessment of possible climatic trends to come.

The existing body of scientific literature that has specifically assessed climate variability for Ottawa, Ontario, Canada, and surrounding area, is limited (e.g., [14–18]). Of these studies, ref. [18] focused less directly on climate trends and more on the effect of general

climate warming as a possible influence on insect populations in the Ottawa area. The other studies variously noted trends such as an increase in wet and humid conditions [14]; seasonal increases in daily minimum temperature values, as well as seasonal variation in daily maximum temperature trends [17]; the attribution of the urban heat island effect as a cause of observed winter warming in Ottawa when contrasted with smaller surrounding communities [15]; and decreased fluvial discharge throughout the Ottawa area [16]. Coverage of the potential impact of climate change has received considerable local media attention though (e.g., Ottawa Citizen newspaper [19]; Canadian Broadcasting Corporation [20]), as well as attention from the City of Ottawa's planning and development division, which has developed a Climate Change Master Plan [21]. This plan focuses on lowering greenhouse gas emissions and encouraging sustainable development as a contribution to combatting global climate change.

Though there have been previous studies on several distinct aspects of climate in Ottawa, these analyses are somewhat scattered and generally do not provide syntheses of the many interactive components of the local climate. The objective of this study is to provide a systematic historical overview of observed trends and cycles in Ottawa's instrumental climate record through the past 130 years (1890–2019) by reviewing several important climate variables, with a focus on synthesizing the results. Specifically, the research assesses (1) trends in temperature and precipitation; (2) environmental responses, specifically the length of the growing season and number of frost-free days, as well as the local fluvial discharge; and (3) trends in extreme weather. Such data will be of considerable use to policymakers and planners as they determine what changes to Ottawa's infrastructure need to be made to make the city more resilient and better able to respond to current and future effects of climate change.

2. Climatic Setting

Ottawa, located in eastern Ontario (45° N, 76° W; Figure 1a), is characterized by a humid continental climate, having warm, humid summers and cold, snowy winters. The regional climate in this part of North America is influenced by trends and cycles at annual and/or seasonal scales and are characterized by patterns driven by the interaction of several climatic oscillations. These include the Schwabe solar cycle (SSC), Atlantic Multidecadal Oscillation (AMO), North Atlantic Oscillation (NAO), Arctic Oscillation (AO), El Niño Southern Oscillation (ENSO), and the Quasi-Biennial Oscillation (QBO) [22–27]. Each of these oscillations and their influence on the climate of eastern North America are described in Table 1.



Figure 1. (a) Location of Ottawa, ON within Canada. (b) Locations of Belleville, ON, Morrisburg, ON, and Chelsea, QC, with respect to Ottawa, ON.

Table 1. Descriptions and regional effects of various climatic oscillations known to impact the region (eastern North America) Ottawa, ON is situated in.

Climatic Oscillation	Notation	Cycle Length (Years)	Description	Common Impact on Eastern North American Climate	Citations
Schwabe Solar Cycle	SSC	~11, 8–17	An oscillation in the annual number of sunspots occurring, relating to total solar irradiance. The increases in total solar irradiance and UV irradiance during sunspot maxima drive dynamic changes in global stratospheric and tropospheric temperatures.	Increases in temperature during sunspot maxima, decreases in temperature during sunspot minima. Various links to precipitation and precipitation-related parameters.	[28–31]
Atlantic Multidecadal Oscillation	AMO	~64, 50–90, 16–24 subharmonics	An oscillation in the circulation pattern of warm and cool Atlantic Ocean surface waters. Warm (AMO+) phases occurred from ~1925–1965 and ~1990–present, cool (AMO–) phases occurred from ~1900–1925 and ~1965–1990.	AMO+ is associated with increased temperatures, decreased precipitation, and greater drought probability.	[32–39]
North Atlantic Oscillation	NAO	poorly defined, typically subdecadal–interdecadal	A localized oscillation in the sea level pressure differential between the Azores High and the Icelandic Low in the northern Atlantic Ocean.	NAO+ phases are typically associated with more moderate temperatures and wetter conditions in eastern North America, and drier, more extreme temperatures during NAO phases.	[40–43]
Arctic Oscillation	AO	poorly defined, typically subdecadal–interdecadal	A broad oscillation in sea-level pressure in the Northern Hemisphere, occurring in an annular band around the northern midlatitudes. During its positive phase, the AO supports a low-amplitude jet stream; during an AO- phase the jet stream becomes a high amplitude waveform. The localized NAO is a constituent of the broad-scale AO.	Brings cool Arctic air to the mid-latitudes during AO+; cool Arctic airmasses travel further south into North America during AO-.	[44–47]
El Niño Southern Oscillation	ENSO	2–10	An oscillation characterized by the changes in sea surface temperatures in the tropical Pacific. Driven by the variation in strength of tropical trade winds—causing greater or weaker degrees in the upwelling of cool, deep ocean water during El Niño (ENSO+) and La Niña (ENSO-), respectively—this oscillation influences many regions of the world via various global interactions.	Warmer, drier conditions during El Niño; cooler, wetter conditions during La Niña.	[48–52]
Quasi-Biennial Oscillation	QBO	2.1–2.4	The oscillation between westerly and easterly winds in the equatorial stratosphere. Air masses then propagate downward to the troposphere and are subsequently propagated poleward via interactions with surface waves.	Cooler temperatures during the westerly (QBO+) phase, warmer temperatures during the easterly (QBO–) phase.	[53–59]

As of 2019, the population of the Ottawa-Gatineau Metropolitan Area was 1.48 million [60]. As urban areas increase in size and population, the development of a heat island effect, where due to an increase in sunlight absorbing paved areas and percentage of area covered by buildings, urban areas tend to be warmer than the surrounding rural areas. This effect has been previously studied in several Canadian cities, including Ottawa [15,16], Montreal, Toronto, and Vancouver, and across the globe [61–63].

3. Methods

Daily resolution climate data for Ottawa was retrieved from [64] with data spanning from 1890–2019 with 98.9% data availability. This record contains information pertaining to daily minimum and maximum temperatures and precipitation in the form of rainfall and snowfall.

Time series data based on daily weather records contain high-frequency noise, which was smoothed by variously computing a mean annual value for temperature and by summing the precipitation for each year. This smoothing procedure was also carried out on a seasonal basis by dividing the daily weather record into meteorological seasons (winter (DJF), spring (MAM), summer (JJA), autumn (SON)), then applying the averaging or summations. Locally weighted regressions (LOWESS; [65,66]) were carried out over 20-year periods for each of the annual and seasonal average maximum and minimum temperatures, and the annual and seasonal rainfall and snowfall totals. LOWESS smoothing provides a clearer assessment of the long-term changes in these long-running time series data sets. The 95% confidence intervals were computed using bootstrap resampling (1000 iterations).

To assess the potential impact of the urban heat island effect (UHIE) in Ottawa, similar data were obtained and processed on a seasonal basis for three additional nearby lesser-urbanized locations (Figure 1b): Chelsea, QC (20 km N, population 6900; [67]), Belleville, ON (190 km SW; population 50,000; [68]), and Morrisburg, ON (70 km S; population 2300; [69]). These three additional communities are considerably smaller than Ottawa but are climatologically similar [70]. Seasonal regressions of maximum and minimum temperatures were carried out for each of the three additional locations. These regressions were then compared to the corresponding Ottawa regressions using a t-value for comparing slopes [71]. Any significant positive differences between stations would indicate that Ottawa is warming faster than surrounding areas and implicate UHIE as a contributor to climate change in Ottawa.

To assess the day-to-day dynamics in temperatures, the diurnal temperature range (DTR) was computed as the difference between daily maximum and minimum temperature on both an annual and seasonal basis. LOWESS smoothing was also performed on the DTR records.

Environmental changes, including the length of the growing season, the number of frost-free days, and discharge for the Ottawa and Rideau rivers, were each analyzed on an annual basis. The length of the growing season and the number of frost-free days each year were derived from Ottawa's minimum temperature record. The start of the growing season was defined as the first span of five days where the minimum temperature was greater than 5 °C, and the end of the growing season was defined as the first span of five days (after the beginning of the season) where the minimum temperature was less than 5 °C [72,73]. A frost-free day is observed when the daily minimum temperature is greater than 0 °C [74]. LOWESS smoothing was carried out for the annual time series of growing season length and number of frost-free days. Data on river discharge was obtained from the [75] via the hydrometric monitoring stations on the Ottawa River and the Rideau River. Annual averages were computed for the discharge data from each river and plotted along with their respective LOWESS models. This information was then compared to that of total annual precipitation input in the Ottawa area using Pearson's correlation coefficient.

Extreme weather was analyzed based on the 95th percentile definition; when the mean of all weather events was considered, anything beyond two standard deviations from the mean was considered to be extreme [76,77]. This analysis was carried out only at

the seasonal resolution to better assess patterns within the record of annual-scale extreme events. The means and standard deviations for temperature (maximum and minimum) and precipitation (rainfall and snowfall) was computed for each season, and the number of extreme events were tabulated for each year. Only non-zero precipitation days were used to calculate means and standard deviations to minimize skewing of the rainfall and snowfall event distributions. While some studies of extreme weather in the region have used a similar methodology (e.g., [78]), other works have defined extreme events in a different manner. For example, ref. [17] specifically examined Ottawa extreme temperature trends as part of their regional Ontario study but defined extreme high and low temperatures as the per annum highest and lowest daily mean recorded temperatures.

For precipitation, a common approach is to combine rainfall and snowfall into a single data type. Precipitation can be binned in discrete intervals (e.g., frequency of rainfall events totaling 0–10 mm, 10–20 mm, etc.; [79]). This approach is commonly used in regions where precipitation patterns are influenced by monsoons. The advantage of using the 95th-percentile definition as used here is that it permits a more nuanced analysis of extreme weather trends, most notably by making it possible to distinguish seasonal variations in long-term trends. This approach also makes it much easier to compare results obtained from multiple locations where different climate conditions exist (e.g., arid vs. humid conditions). LOWESS smoothing was carried out for the discrete counts of extreme weather events.

For each of the annual, seasonal, and extreme weather records described above, spectral analyses were performed to determine whether there were any periodic (cyclic) components within each time series. The methodology employed included red noise spectral analysis [80], which is based on Thomson's multitaper power spectrum estimate [81] and uses chi-squared and Monte Carlo methods to estimate red noise and confidence levels [82]. This analytical approach converts time-domain data into the frequency domain, quantifying the various cycles that make up a time series. This method provides discrete peaks in the frequency data for simple interpretation, though it carries the assumption that any contained cyclicity is stationary and not intermittent. Continuous wavelet transforms (CWTs) provide the same time-frequency transformation as obtained through red noise spectral analysis, but this method assumes that there are non-stationary data components. Thus, CWTs permit the recognition of changes in frequency information over time [83]. In contrast to red noise spectral analysis, CWTs are not accompanied by discrete peaks, though. Due to the complementary nature of spectral and CWT analysis, these two methods are often used in tandem (e.g., [62,84]).

In addition, cross wavelet transforms (XWTs) were carried out to compare the annual, seasonal, and extreme weather records with several natural climate phenomena that are known to influence the Ottawa regional climate. Cross wavelet analysis, as described in [83], is similar to continuous wavelet analysis in that recorded time series are analyzed for the presence of periodic signals and their variation through time. However, XWTs process the time domain to frequency domain transformation for two time series (a reference signal and an analyte signal) and compare the time-frequency information within each series. Similar to statistical correlations obtained when comparing linear data sets, XWTs are used to reveal any relationships between the periodic elements contained within two time series. Here, the reference signals were the historical annual, seasonal, and extreme weather records, and the analyte signals were the quantitative records of the SSC [85], AMO [86], NAO [87], AO [88], ENSO [89], and QBO [90].

4. Results

4.1. Long-Term Climate Changes

4.1.1. Temperature and Precipitation

Ottawa's temperature and precipitation record has significantly changed since record-keeping began in 1890 (Figure 2). The annual average maximum and minimum temperatures have generally increased, albeit with periodic reversals through that interval, a trend that has been more pronounced for minimum temperatures. The minimum temperature

has risen fairly steadily since ~1950, whereas maximum temperature shows a sharper rise after 1980, peaking around 2010. Through the entire 130 years span of the data analyzed, the annual average maximum temperature has increased by $1.3 \pm 0.2 \text{ }^\circ\text{C}$, and the annual average minimum temperature has increased by $2.3 \pm 0.2 \text{ }^\circ\text{C}$. Seasonally, changes in maximum temperature have occurred most strongly during winter ($+1.7 \pm 0.3 \text{ }^\circ\text{C}$ since 1890) and least strongly during spring ($+0.7 \pm 0.5 \text{ }^\circ\text{C}$; Figure 3, Table S1). Minimum temperature changes were significant in each season, with summer and autumn having the smallest increases ($1.5 \pm 0.2 \text{ }^\circ\text{C}$ and $1.8 \pm 0.3 \text{ }^\circ\text{C}$) and winter having the strongest change ($3.0 \pm 0.2 \text{ }^\circ\text{C}$) since 1890. Many of the annual and seasonal maximum and minimum temperature records peak in the 2000–2010 span before decreasing slightly in the 2010s.

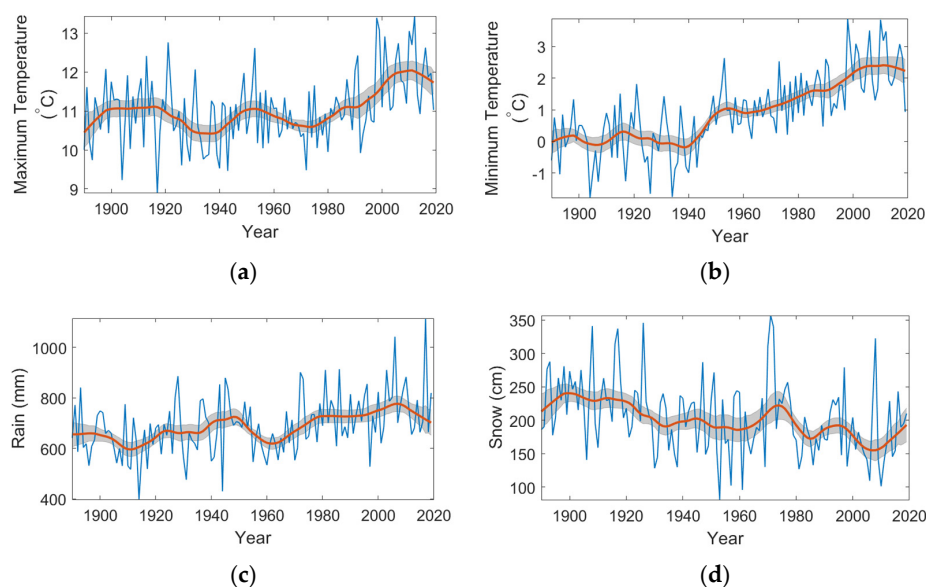


Figure 2. Smoothed (LOWESS, span $0.15 \pm 95\%$) plots for (a), annual average maximum temperature, (b) annual average minimum temperature, (c) annual rainfall totals, and (d) annual snowfall totals.

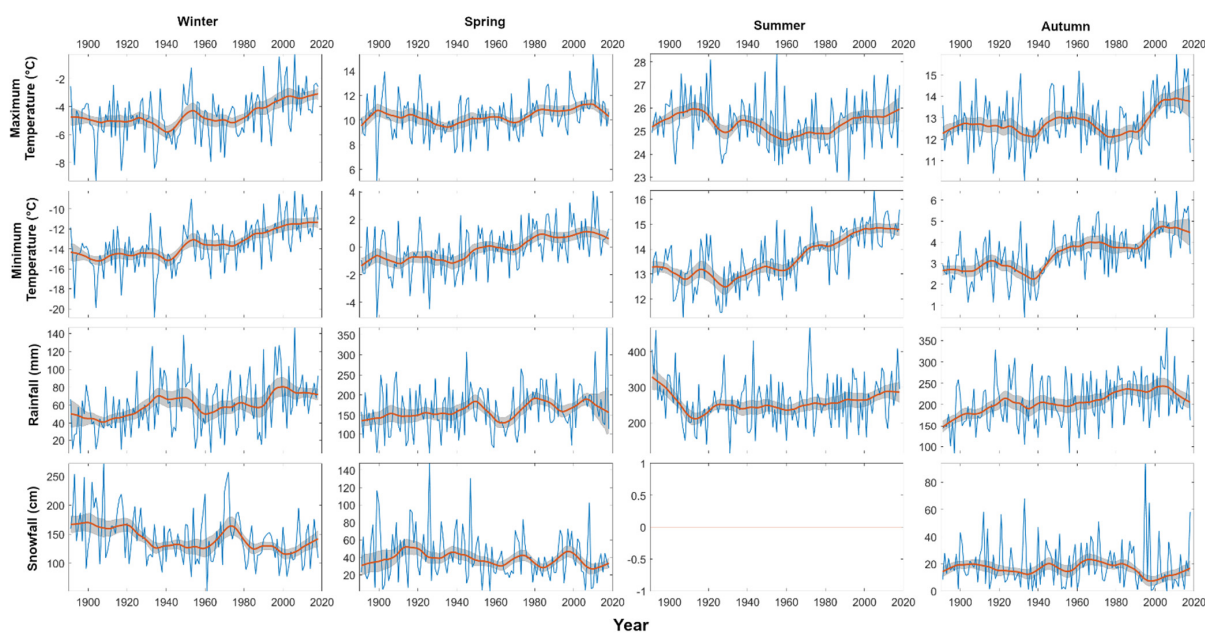


Figure 3. Smoothed (LOWESS, span $0.15 \pm 95\%$) plots for the seasonal climate time-series for Ottawa, Canada.

Annual rainfall and snowfall totals have exhibited opposite trends through the 1890–2019 interval with annual rainfall totals increasing by 46.3 ± 35.3 mm, and snowfall totals decreasing by 20.1 ± 18.2 cm, due to the shift toward warmer conditions during the colder months when precipitation that previously fell as snow subsequently fell as rain (Figure 2). Figure 4 also depicts this information as a ratio of rainfall to snowfall, which shows a clear increase in this ratio over time. Seasonally, summer rainfall has shown the steadiest trend through the past 130 years (with the exception of a substantial decrease from ~1890–1920), whereas autumn is characterized by the greatest increase, followed by smaller increases in winter and spring (58.3 ± 16.3 mm, 21.5 ± 8.1 mm, and 20.6 ± 28.0 mm, respectively; Figure 3 and Table S1). Seasonal snowfall changes since 1890 occurred most strongly during winter (-4.9 ± 9.6 cm) and minimally in spring (2.8 ± 6.2 cm) and autumn (2.5 ± 3.4 cm). As with the temperature records, both annual and seasonal rainfall (snowfall) records peaked (troughed) between 2000–2010 and decreased (increased) in the 2010s.

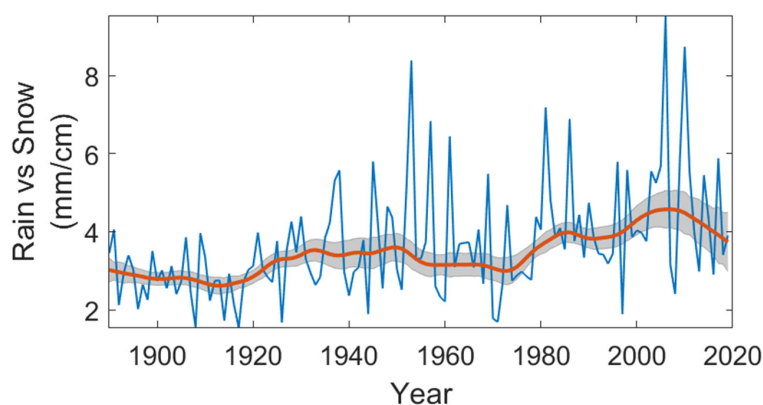


Figure 4. Smoothed (LOWESS, span $0.15 \pm 95\%$) plots for the ratio of annual rainfall total (mm) to annual snowfall total (cm).

4.1.2. Diurnal Temperature Range (DTR)

The trends in DTR are shown on both an annual (Figure 5) and seasonal (Figure 6) basis. Since 1890, DTR has decreased on an annual basis by 1.0 ± 0.2 °C. This decrease is more notably pronounced in the winter and spring, where decreases in range of 1.3 ± 0.4 °C and 1.2 ± 0.3 °C are observed, respectively. In contrast, the DTR during the summer and autumn seasons has decreased by only 0.4 ± 0.3 °C and 0.2 ± 0.3 °C. Also of particular note is that annually and mainly in summer and autumn, there is a common trend where the DTR increased from approximately 1890 to 1910 and then decreased until approximately 1980. Since then, the DTR in annual, summer, and autumn records have slightly increased.

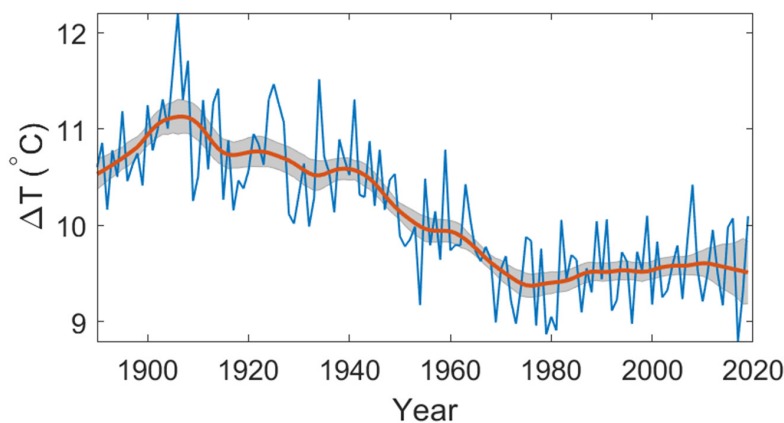


Figure 5. Smoothed (LOWESS, span $0.15 \pm 95\%$) plot for the diurnal temperature range (DTR).

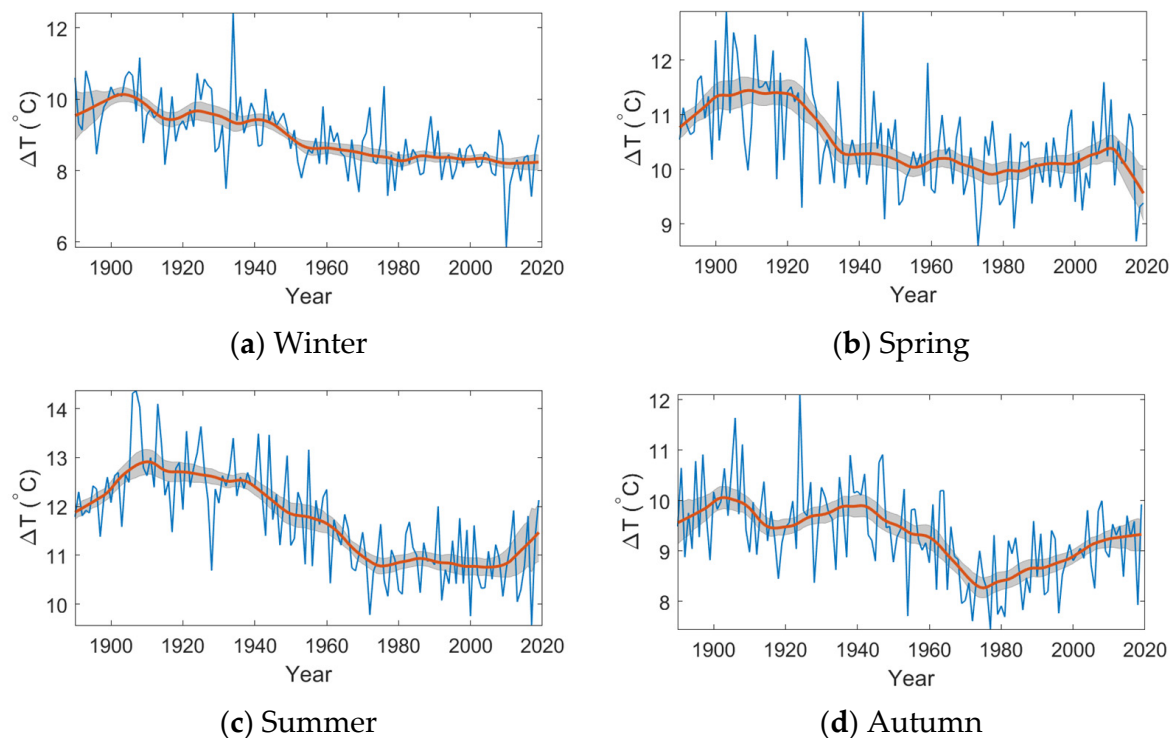


Figure 6. Smoothed (LOWESS, span $0.15 \pm 95\%$) plots for seasonal, diurnal temperature range (DTR).

4.1.3. Comparing Ottawa Temperature Trends to Lesser or Non-Urban Areas

The maximum and minimum temperature difference (ΔT) between Ottawa and, respectively, for Belleville, Morrisburg, and Chelsea, is shown in Figure 7. In most cases, ΔT maximum/minimum temperature regressions between Ottawa and each of the communities are near-zero to slightly positive (Table S2), indicating that the rate of change within Ottawa's maximum and minimum temperature records are similar to those of Belleville, Morrisburg, and Chelsea. In most cases where these regressions indicate a mild positive trend, the statistical significance at the 95% confidence level is low. Only two of the comparisons of maximum temperature regressions are statistically significant (with opposite signs), and five of the minimum temperature comparisons are significant (with one negative relationship and four positive). The strongest indication of Ottawa temperature having a differing rate of change than surrounding communities for any measured variable is within the summer minimum temperature record, with Ottawa's rate of change being significantly higher than those of Belleville and Chelsea but significantly lower than Morrisburg's.

4.1.4. Changes in Environmental Responses

As suggested by the increases in average annual minimum and maximum temperatures since 1890, the length of the Ottawa growing season and the number of frost-free days have significantly increased by 23.3 ± 4.2 days through the past 130 years (Figure 8). There has also been a sustained increase in the number of frost-free days, particularly since 1950 (Figure 8 and Table S1). In a typical year at present, there are 12.7 ± 3.0 more frost-free days than in 1890, though the average number of frost-free days has declined since ~2010.

4.1.5. Changes in River Discharge

The discharge of both the Ottawa and Rideau rivers has increased dramatically since record-keeping began (Figure 9). Since 1960, the Ottawa River's annual average discharge has increased by $34.7 \pm 0.8\%$ ($360.4 \pm 6.4 \text{ m}^3/\text{s}$), and during the same timeframe, the Rideau River's discharge has increased by $40.6 \pm 1.1\%$ ($13.9 \pm 0.4 \text{ m}^3/\text{s}$). For the total length of the available record for the Rideau River (1933–2018), its discharge has increased by a remarkable $252.4 \pm 4.8\%$ ($34.4 \pm 0.4 \text{ m}^3/\text{s}$). For both rivers, these are substantial

changes and are indicative of a changing environment. It is important to note, though, that both the Ottawa River and Rideau River are subject to active flood management control practices in the spring and autumn. While autumn drawdown and spring flood control measures are observable in the discharge records, this semi-annual pattern does not appear to have influenced the overall increase in river discharge in either of the two rivers.

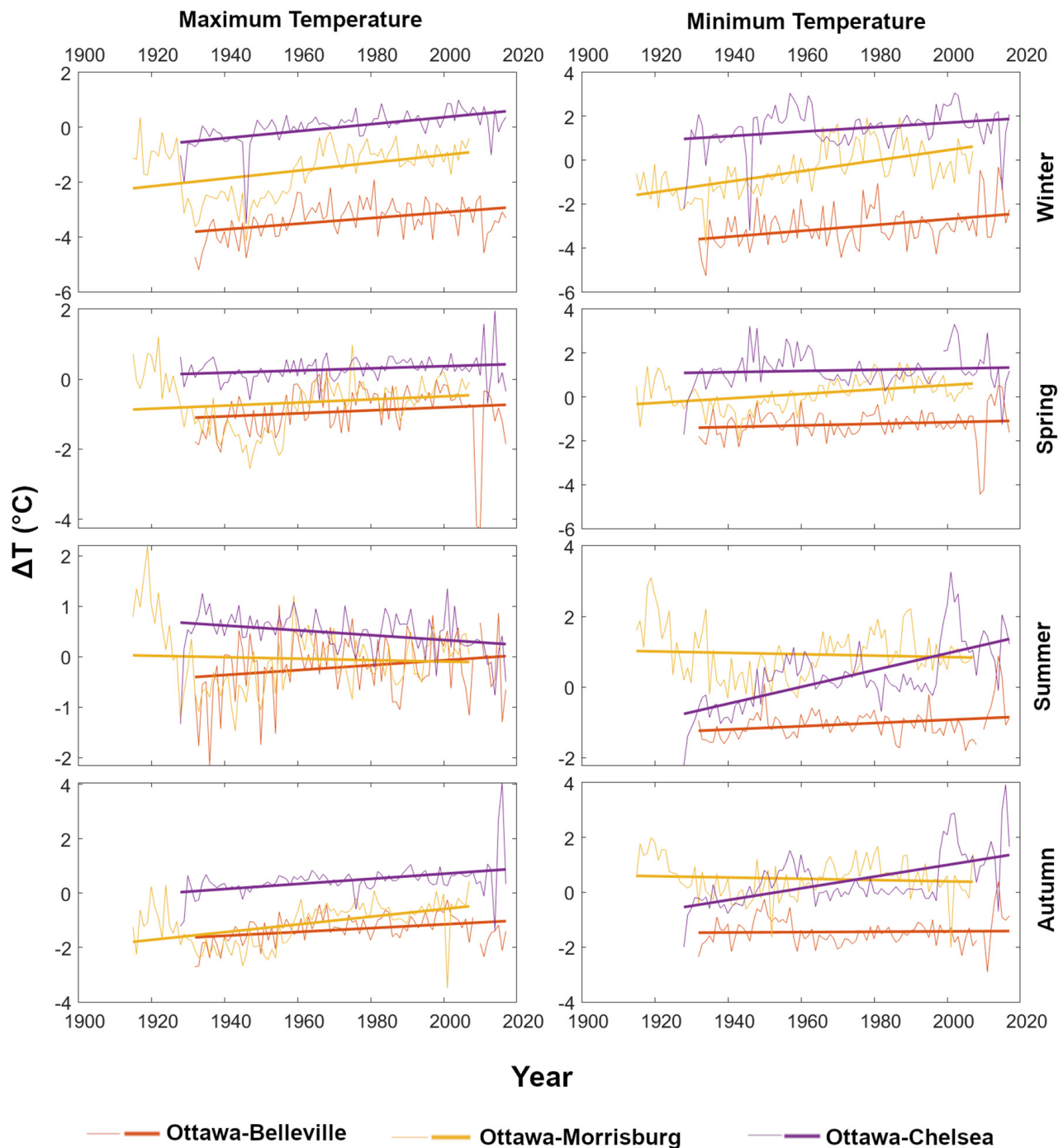


Figure 7. Comparison of maximum and minimum temperature time series between Ottawa and surrounding communities. Each time series/regression is of the daily temperature difference (ΔT) between Ottawa and each of Belleville, Morrisburg (ON), and Chelsea (QC).

Furthermore, the flow rates in both rivers are characterized by a moderate correlation to the total Ottawa precipitation record. An annual sum of the Ottawa total precipitation data was compared to the river discharge data of both rivers via linear correlation. At the 95% confidence interval, this yielded Pearson’s correlation coefficients of 0.49 and 0.62 for the Ottawa and Rideau rivers, respectively, implying that the increase in river discharge in both rivers is moderately related to the increase in precipitation in the region. Additionally, the flow data was recorded on both rivers in Ottawa, near the ends of their catchments. The increase in discharge in both rivers is likely related to increased precipitation and other environmental changes upstream, as well.

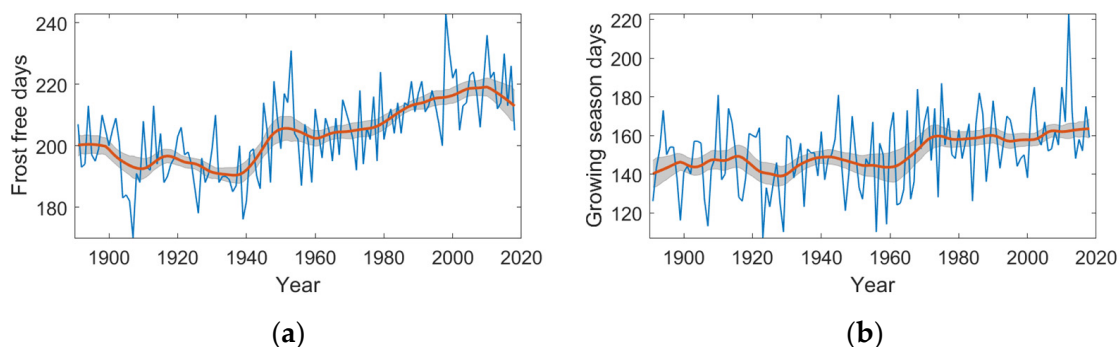


Figure 8. Smoothed (LOWESS, span $0.15 \pm 95\%$) plots for (a) annual number of frost–free days and (b) annual length of the growing season in days.

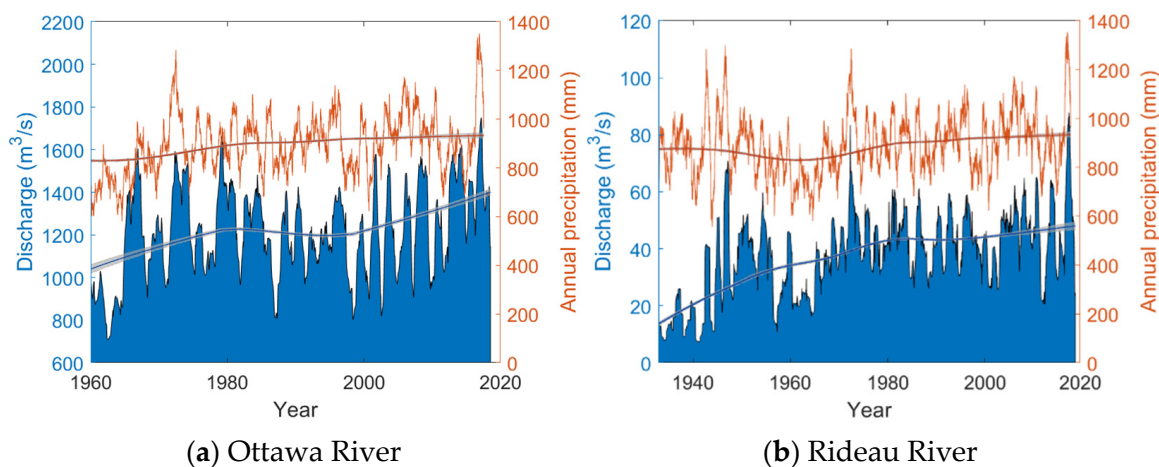


Figure 9. Discharge and water level for the Ottawa and Rideau rivers.

4.1.6. Extreme Weather

Examination of the various extreme weather histograms and their associated smoothed trends indicate relatively small changes over time, with the strongest trends being those describing changes in extreme minimum temperature events (Figure S1 and Table S1). Depending on the season, extreme minimum temperatures in Ottawa have decreased in number by between 1.9 ± 0.5 events (autumn, Table S1) and 0.5 ± 0.9 events (spring). Spring extreme events have generally undergone a stronger decline but underwent an increase from 2010 to 2019). The next strongest of the smoothed extreme weather trends are for extreme maximum temperatures in both spring (2.8 ± 0.4 events) and summer (1.3 ± 0.4 events). It should be noted that the most significant part of the increase in extreme maximum spring and summer temperatures was from ~1980 onward. There have been minimal changes in the periodicity of extreme autumn and winter temperature events.

Changes in the occurrence of extreme precipitation events have undergone relatively minimal change since 1890. The exception to this trend has been the occurrence of extreme autumn rainfall (1.5 ± 0.3 events), which is primarily due to a lack of extreme rain events in the 1890s. There has also been a decrease in the occurrence of extreme winter snowfall through the entire record (-1.3 ± 0.5 events). The observed stability in the occurrence of spring and autumn extreme snowfall is likely due to the lack of consistent snowfall during these shoulder seasons.

4.2. Periodic Patterns in Ottawa Climate

4.2.1. Periodicity in Annual and Seasonal Weather

Annual weather records (maximum/minimum temperature, rain, snow, DTR, growing season length, and frost-free days) are most strongly characterized by ~3–5-year oscillations that occur intermittently throughout the entire 1890–2018 interval (Figures S2 and S3). Cycles of ~8–11 years are also frequent and occur most strongly prior to ~1950, a pattern most apparent in the temperature-related weather variables. A longer period and generally stationary ~20–40-year oscillations are also observed in the annual weather records. Both the frost-free days and growing season length records are characterized by ~30–40-year oscillations. However, for the frost-free days' record, this oscillation is primarily limited to the 1900–1960 window, whereas with the growing season record, this oscillation spans a larger proportion of the record.

Seasonal weather records (maximum/minimum temperature, rain, snow, DTR) are also characterized by strong 3–5-year oscillations (Figure S4). In addition, 2.0–2.5-year and 8–11-year oscillations are particularly common in spring records. Longer period ~20–40-year cycles are also present but are primarily concentrated in summer records. Distinct similarities were observed between the oscillatory components of the seasonal maximum and minimum temperature records, as well as between rainfall and snowfall records. The occurrence of each of the short (<5 years) seasonal oscillations through time was quite variable for each seasonal weather variable, though the 8–11-year oscillations typically occurred at similar times for maximum and minimum temperature records (e.g., Spring ~1980–2010, winter ~1900–1920) and occasionally DTR (e.g., summer ~1900–1940; Figure S5). While rainfall and snowfall generally contained similar oscillatory components, they were not necessarily coherent in their occurrence.

4.2.2. Periodicity in Extreme Weather

Spectral analysis and CWTs for Ottawa's extreme weather records are shown in Figures S6 and S7. Periodicities that varied from 2–8 years were most common throughout each weather variable and season. Less frequently, 10–20-year cycles were observed, as well as some occurrences of ~30, ~40, and ~50-year cycles. The occurrence of 2–8-year cycles are dispersed throughout the record and are non-stationary with no discernable pattern (Figure S6), though the significant 10–20-year cycles occur most often in the early 20th century. Each of these patterns is pervasive in each season.

4.2.3. Cross Wavelet Transforms

Cross wavelet transforms (XWTs) were used to determine which, if any, long-term oscillations that are known to regionally impact climate have relationships with annual, seasonal, and extreme weather patterns in Ottawa. Each annual, seasonal, and extreme weather record was compared against the SSC [85], AMO [86], NAO [87], AO [88], ENSO [89], and QBO [90] (Figures 10–20).

By far, the SSC displays long-running continuous or semi-continuous relationships with the annual, seasonal, and extreme weather variables. Of these variables, SSC had a strong correlation with maximum summer temperature, summer minimum temperature, and DTR prior to ~1940, which weakened considerably in the latter part of the record (Figures 12–14). Rain and snow records (both annual and seasonal) indicate reasonably continuous relationships to the SSC (Figures 10, 15 and 16).

For extreme weather and the SSC, all four of the extreme seasonal variables (i.e., maximum and minimum temperature, snow, and rain) indicate a continuously strong relationship with SSC. Where discontinuities exist, they are dispersed, with no discernable seasonal or extreme weather-type pattern (Figures 17–20).

The AMO has a significantly weaker relationship with the examined Ottawa weather variables than observed with the SSC. The most significant AMO-related periodicities are comprised of ~5-year cycles dispersed intermittently throughout the records (Figures 10–20). However, a common but statistically less significant relationship (below 95% confidence) with an oscillation of ~16–32-years is found in all the annual weather records, which is comparable to previously reported 16–24-year harmonics [42,62]; Figures 10 and 11). This relationship was also found between the AMO and seasonal maximum and minimum temperature records (winter and summer only), and snowfall (all seasons). Correlation between the AMO record and extreme weather is primarily limited to the short intermittent cycles, although the ~16–32-year cyclicity is again observed in these records, particularly with extreme snowfall (Figure 20).

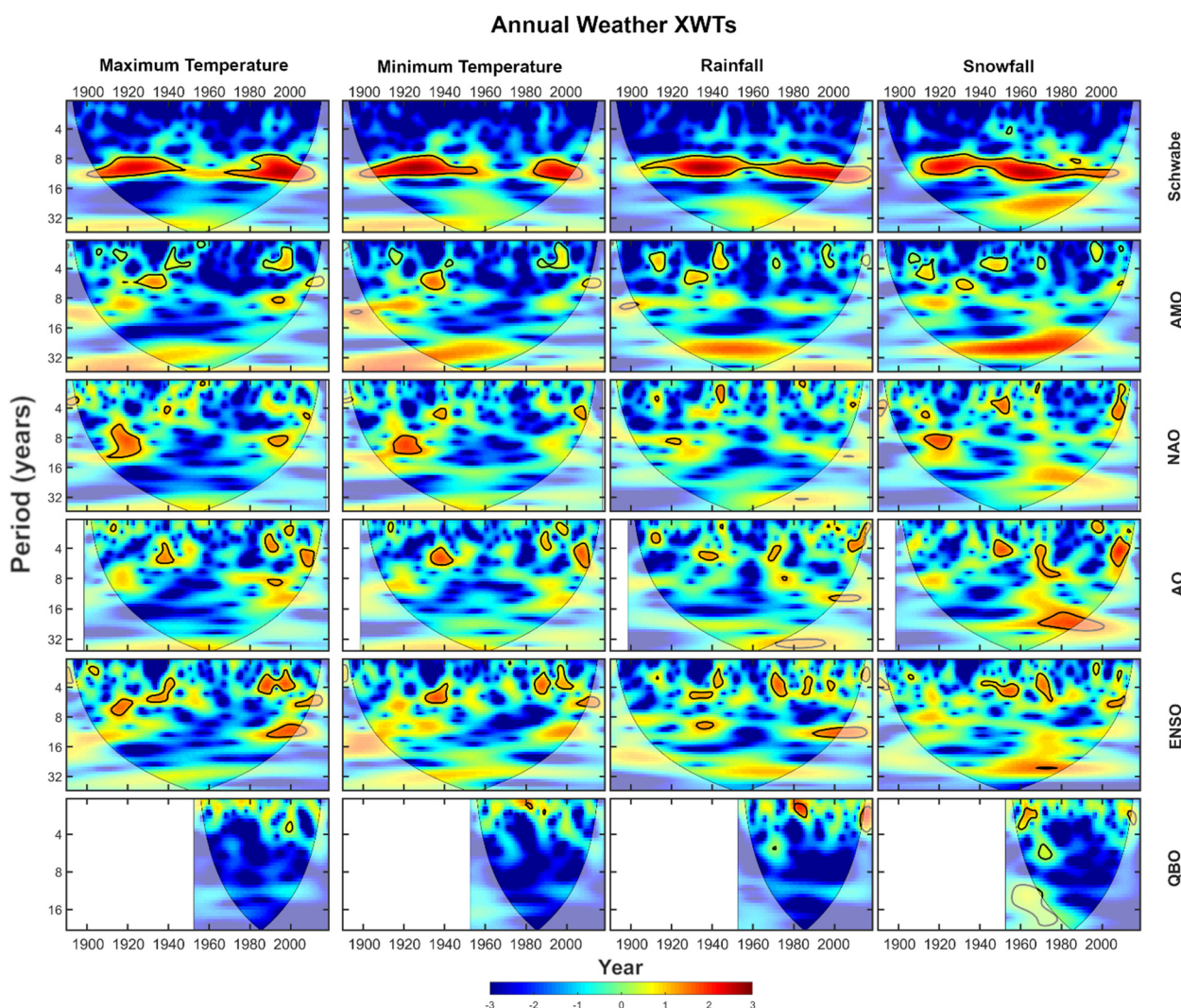


Figure 10. Cross wavelet (XWT) analysis between Ottawa annual maximum and minimum temperatures, rainfall, and snowfall (columns) and six climate phenomena (rows, right y-axis). Areas of high common spectral density that are above the 95% confidence interval are outlined in black.

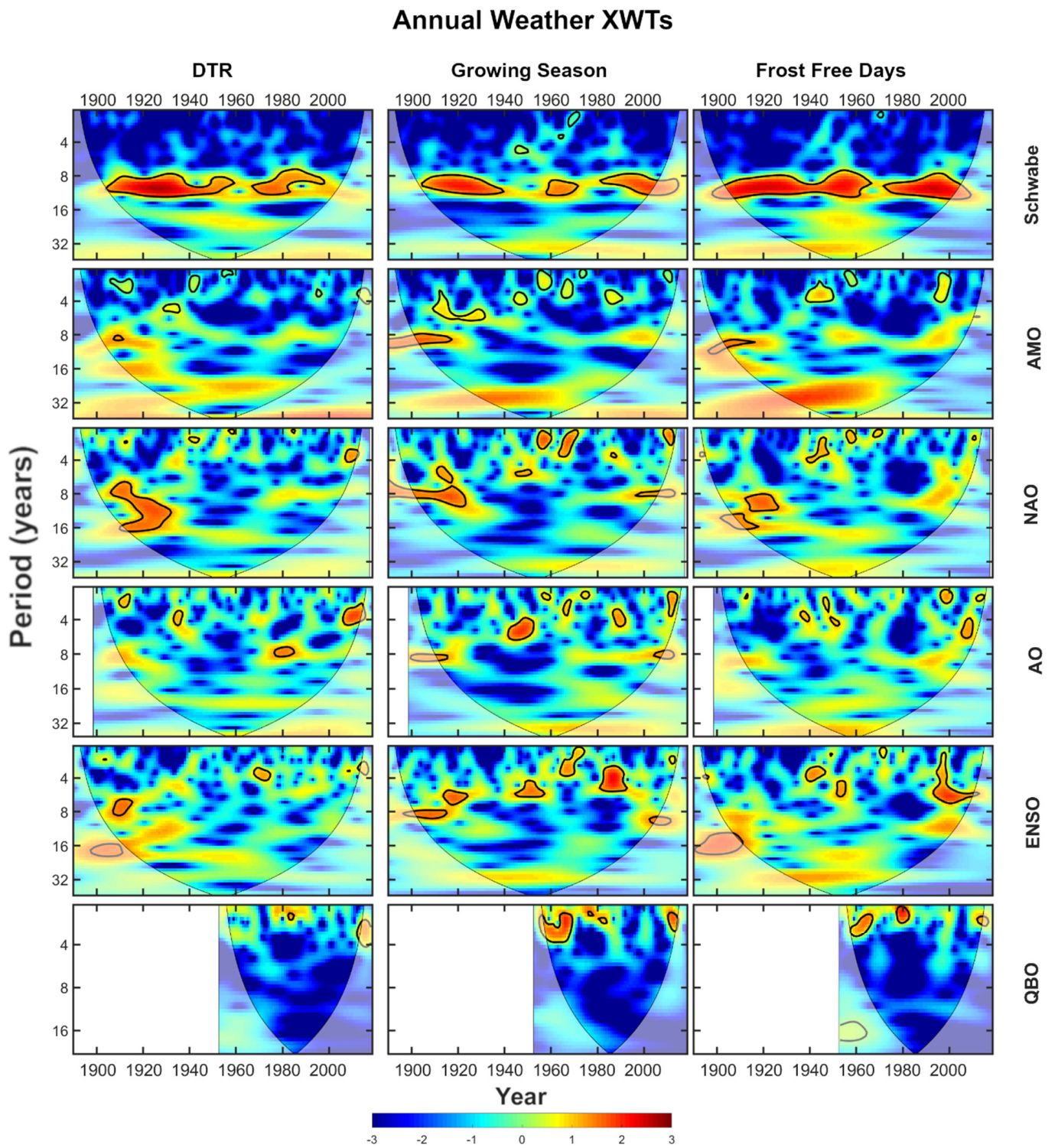


Figure 11. Cross wavelet (XWT) analysis between Ottawa annual diurnal temperature range (DTR), growing season length, and frost-free days (columns) and six climate phenomena (rows, right *y*-axis). Areas of high common spectral density that are above the 95% confidence interval are outlined in black.

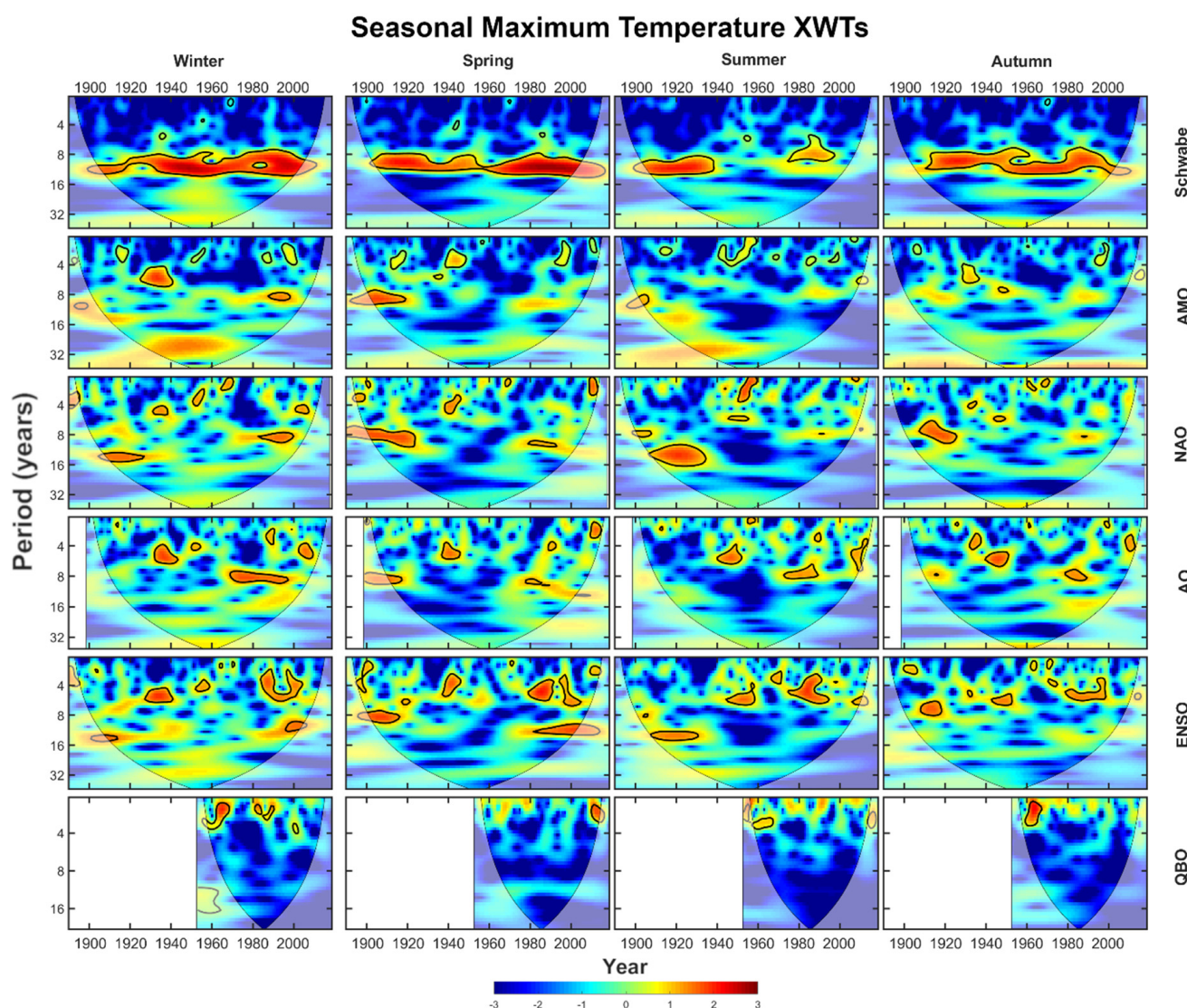


Figure 12. Cross wavelet (XWT) analysis between Ottawa seasonal maximum (columns) and six climate phenomena (rows, right *y*-axis). Areas of high common spectral density that are above the 95% confidence interval are outlined in black.

The records of NAO, AO, and ENSO, despite being distinct phenomena, individually have similar influences on annual maximum temperature, minimum temperature, rainfall, and snowfall patterns in Ottawa (Figure 10). The XWTs between each of these climate drivers and the analyzed temperature and precipitation records are characterized by similar patterns. For example, individual comparisons between the annual minimum temperature record and NAO, AO, and ENSO are characterized by common ~4-year and 4–10-year cycles, centered on ~1940 and ~1990–2010, respectively.

This relationship was also prevalent with seasonal and extreme weather records (e.g., winter minimum temperature, Figure 13; spring extreme maximum temperature, Figure 17). The NAO, AO, and ENSO also exhibited very strong relationships with both extreme maximum and minimum temperature (Figures 17 and 18), but only weak to moderate correlations with the rest of the analyzed seasonal and extreme weather records. There was a greater distinction between the NAO, AO, and ENSO influences (e.g., growing season length, frost-free days, and both annual and seasonal DTR were characterized by more distinct patterns in their interactions with the NAO, AO, and ENSO; Figures 11 and 14). Overall, the AO had the weakest influence, with NAO and ENSO having a more significant influence on these variables.

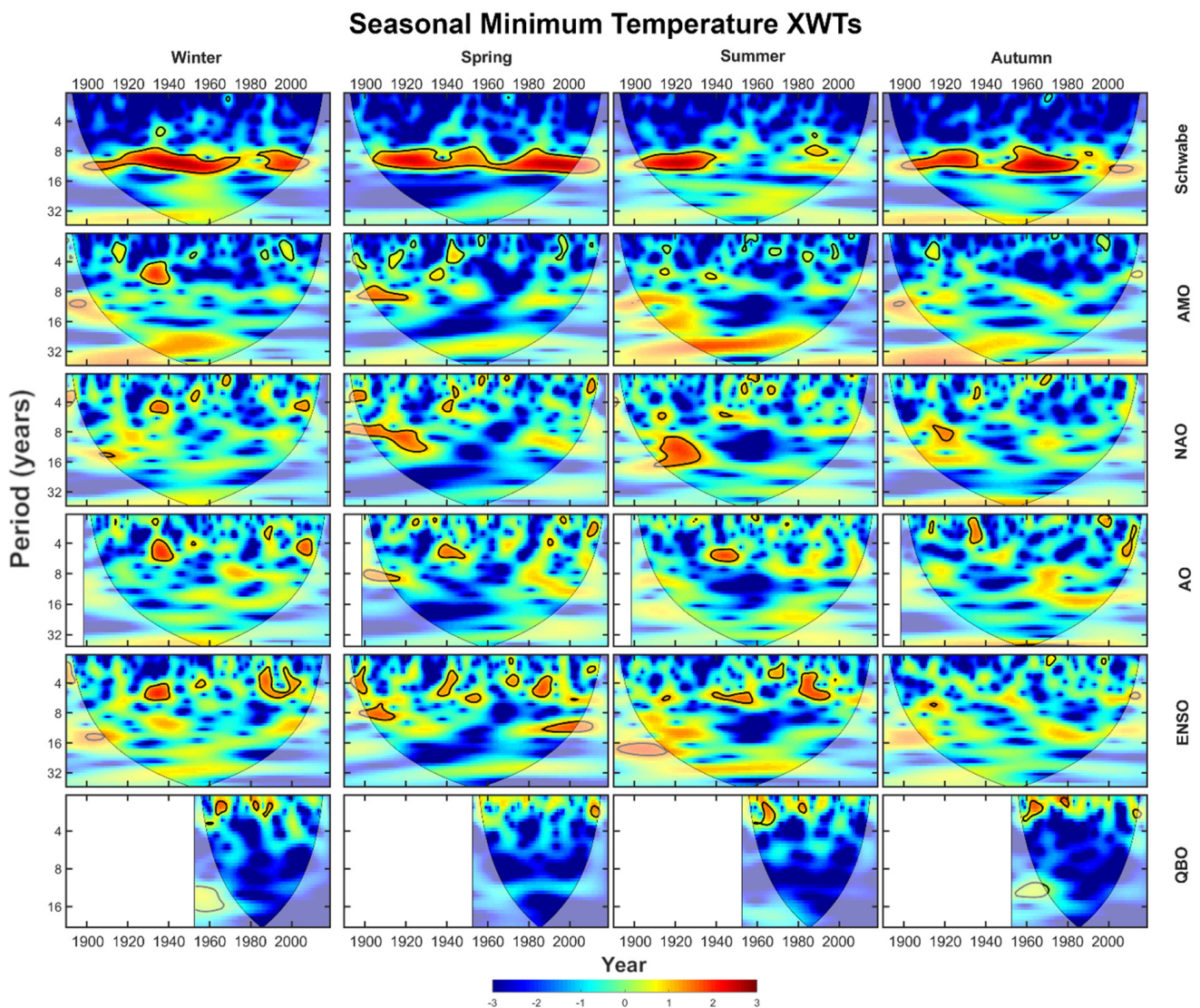


Figure 13. Cross wavelet (XWT) analysis between Ottawa seasonal minimum temperature (columns) and six climate phenomena (rows, right *y*-axis). Areas of high common spectral density that are above the 95% confidence interval are outlined in black.

When examining these instances of NAO-AO-ENSO relationships with annual and seasonal weather, several peaks in the weather records are observable, indicating warmer or wetter conditions (e.g., spring/summer maximum and minimum temperatures, ~1920; winter maximum and minimum temperatures, the late 1990s, Figure 3). Particular phase relationships between the NAO, AO, and ENSO can be identified from the indices of the climate oscillations (Hurrell and NCAR, 2020; NCAR, 2020; Trenberth and NCAR, 2020) when examining these peaks in annual and seasonal weather, suggesting an increased likelihood of warmer or wetter years during certain phase combinations. For example, NAO+, AO+, and ENSO- tend to typify warmer annual and seasonal temperatures compared to other phase combinations (e.g., ~1920 and late ~1990s), whereas instances of NAO+, AO+, and ENSO+ result in wetter periods (e.g., autumn rain, ~1915; spring/summer rain and winter/spring snow, early 1970s; Figure 3).

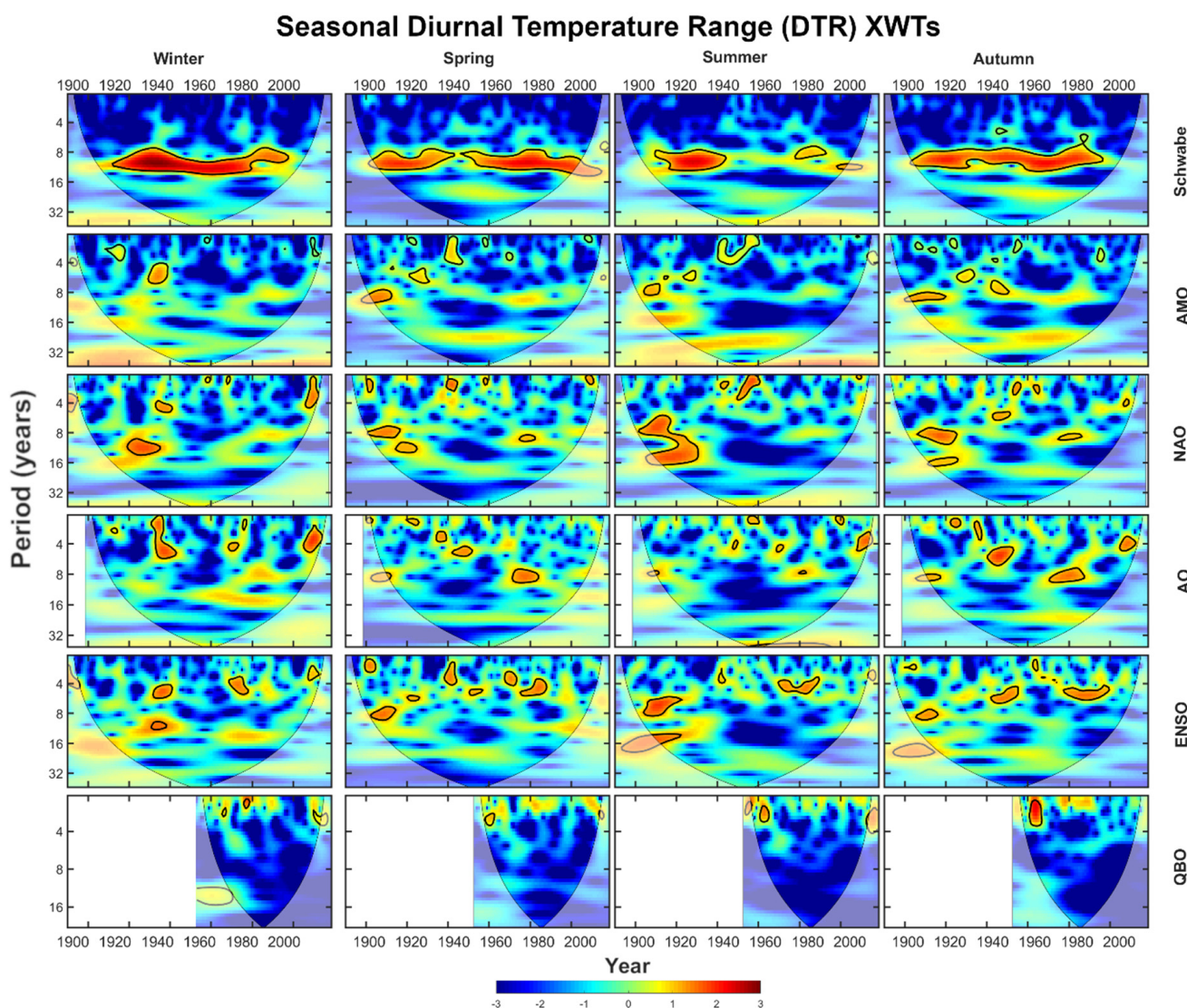


Figure 14. Cross wavelet (XWT) analysis between Ottawa seasonal, diurnal temperature range (DTR) (columns) and six climate phenomena (rows, right y-axis). Areas of high common spectral density that are above the 95% confidence interval are outlined in black.

Both extreme maximum and minimum temperatures are characterized by distinct discontinuous relationships with the AMO, NAO, AO, and ENSO records, particularly in winter. For extreme maximum temperature, this discontinuity occurred in the ~1960–1970 interval, after which the relationship between maximum and minimum temperature and the AMO, NAO, AO, and ENSO climate drivers strengthened. A similar pattern was observed with the spring maximum and minimum temperature records, though rather than there being just one discontinuity being present in the ~1960–1970 interval as observed with the winter record, there was an additional discontinuity at ~1920. Furthermore, the strength of the association between AMO, NAO, AO, and ENSO and extreme maximum and minimum spring temperatures between ~1920 and 1970 was relatively weak compared to the winter record.

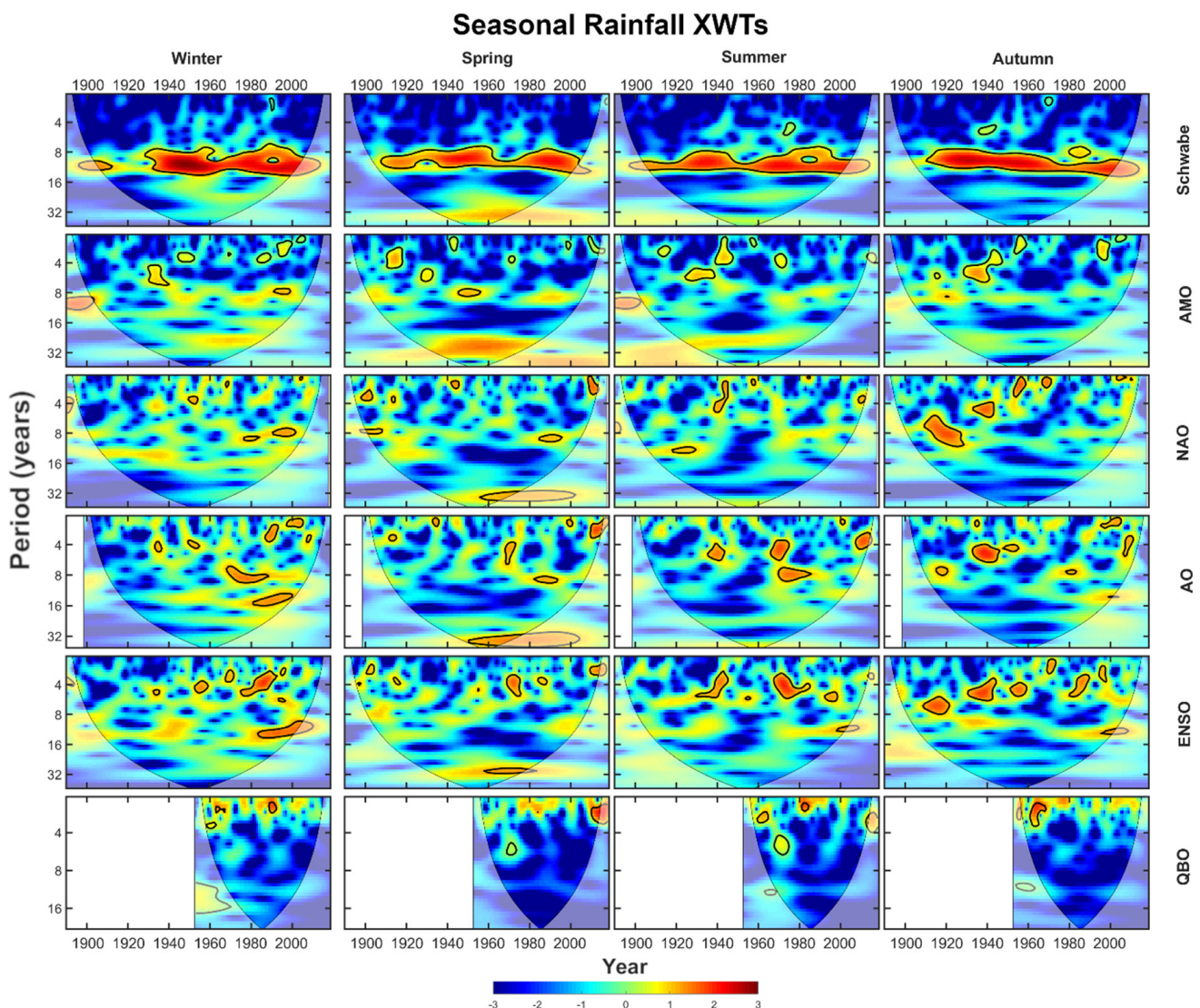


Figure 15. Cross wavelet (XWT) analysis between Ottawa seasonal rainfall (columns) and six climate phenomena (rows, right y -axis). Areas of high common spectral density that are above the 95% confidence interval are outlined in black.

The QBO exhibited a weak to moderate and intermittent influence on weather patterns in Ottawa. In general, the XWT cycles based on the QBO data were typically 2–3 years in length, although there was also an 8–16-year cycle present between the 1950s–1980s for some seasonal level QBO derived XWTs (e.g., winter, spring, and autumn extreme maximum temperature, Figure 17). By and large, the relationship between QBO and the assessed weather variables was strongest with seasonal extreme maximum and minimum temperatures and extreme rainfall records (Figures 17–19), as well as seasonal temperature, precipitation, and DTR records (Figures 12–16), and the annual growing season and frost-free days records (Figure 11). Annual-scale temperature and precipitation records (including DTR) generally exhibited comparatively weaker relationships with QBO (Figures 10 and 11).

Seasonal Snowfall XWTs

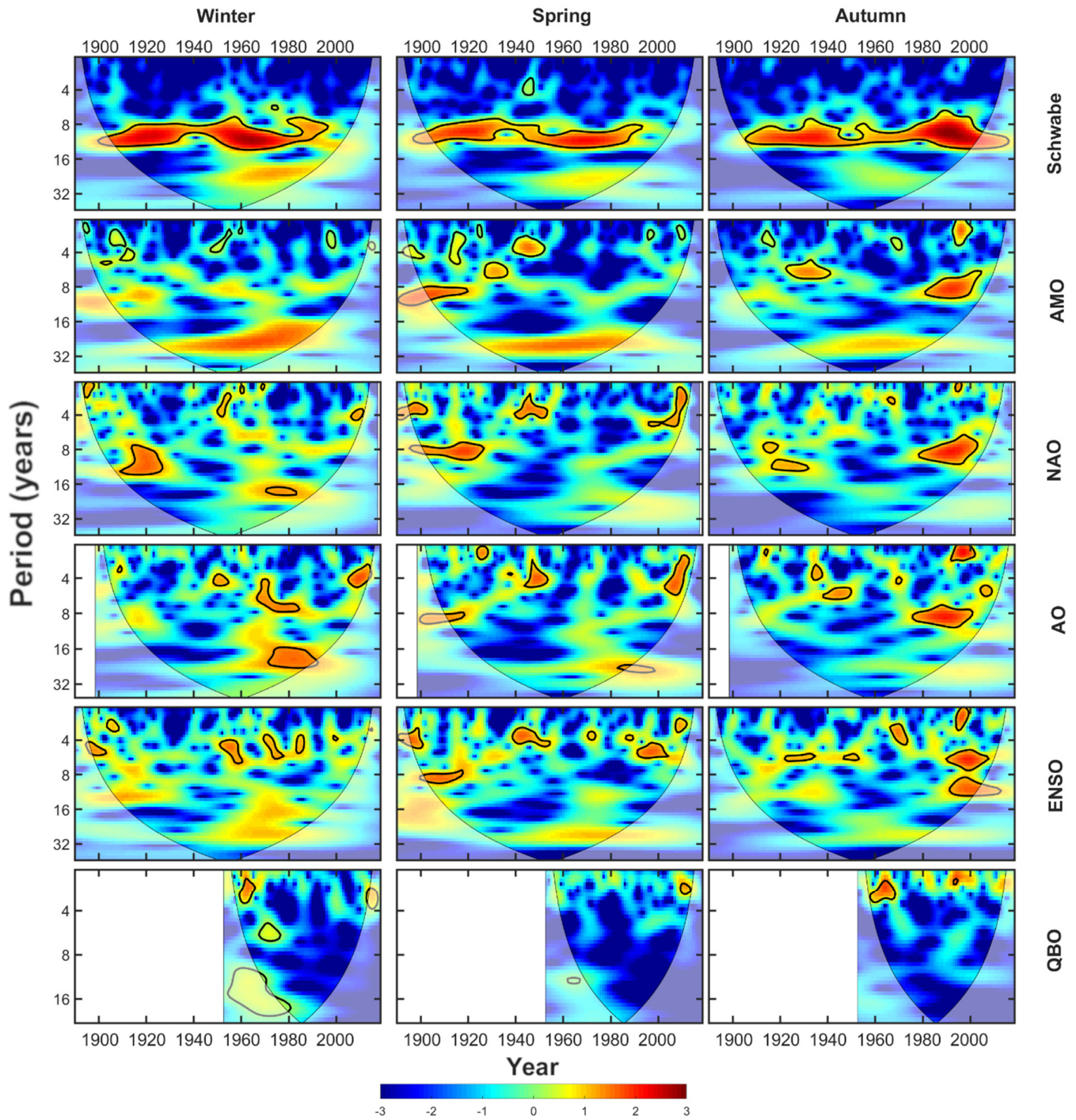


Figure 16. Cross wavelet (XWT) analysis between Ottawa seasonal snowfall (columns) and six climate phenomena (rows, right y-axis). Areas of high common spectral density that are above the 95% confidence interval are outlined in black.

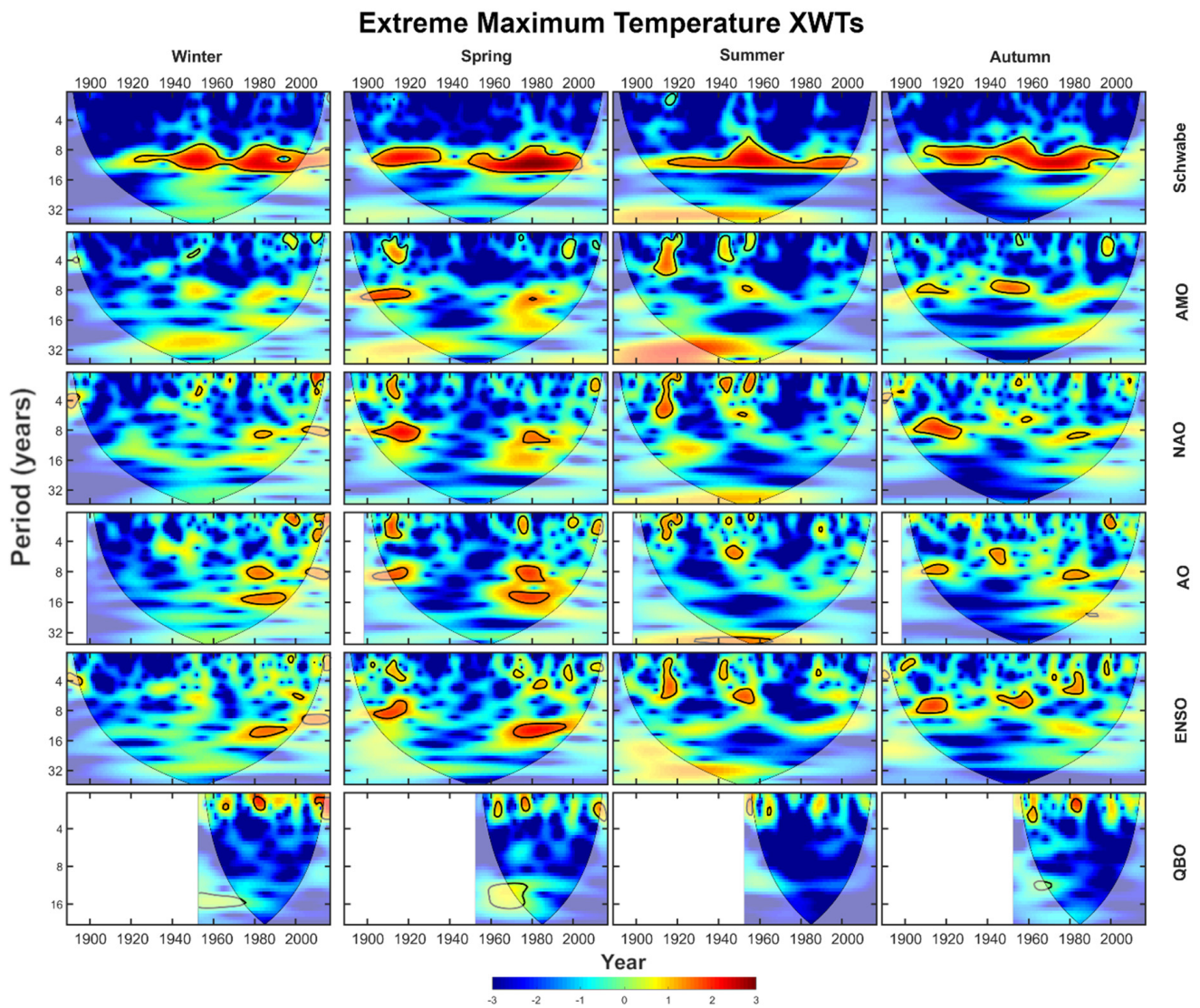


Figure 17. Cross wavelet (XWT) analysis between Ottawa extreme maximum temperature (columns) and six climate phenomena (rows, right y -axis). Areas of high common spectral density that are above the 95% confidence interval are outlined in black.

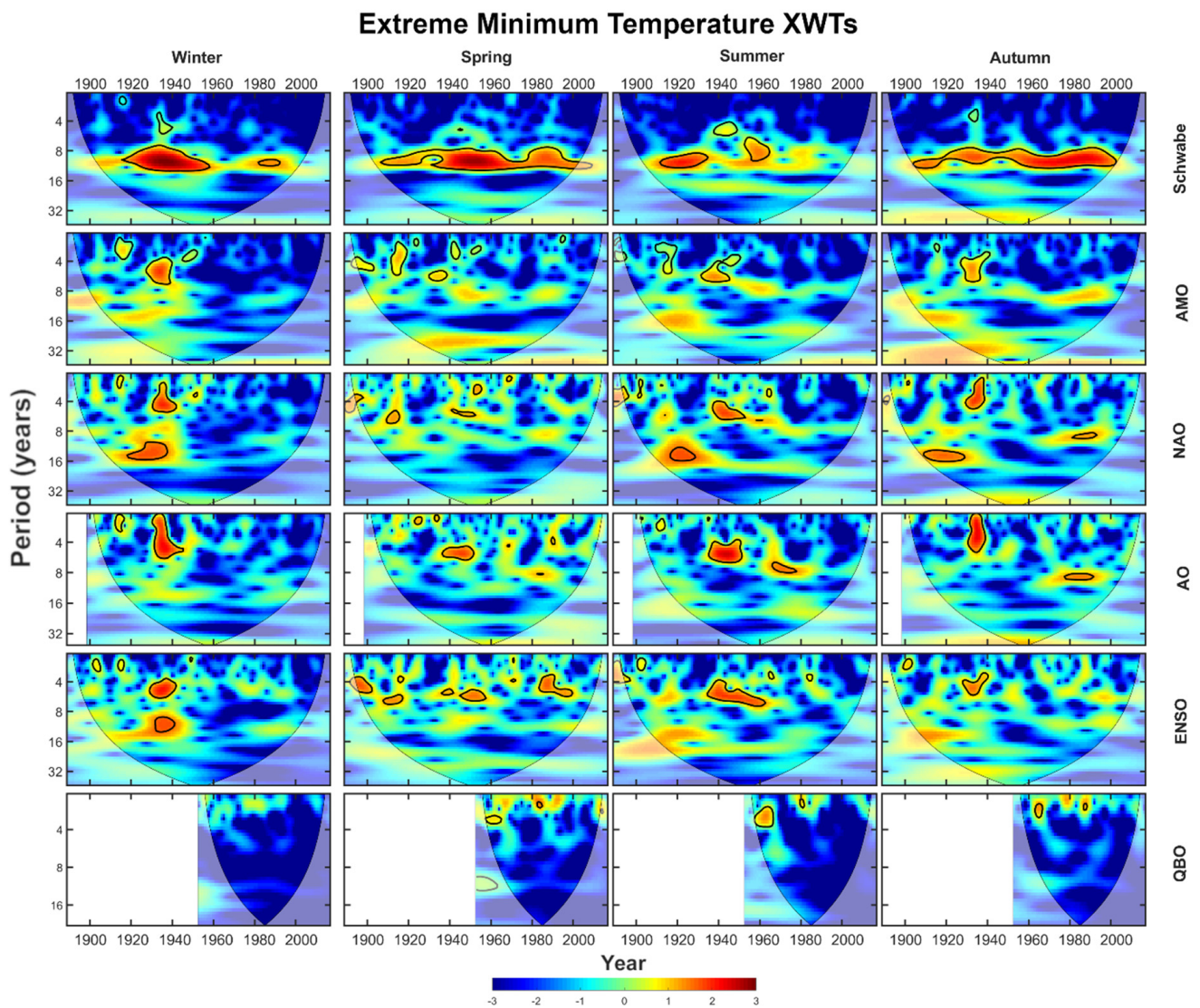


Figure 18. Cross wavelet (XWT) analysis between Ottawa extreme minimum temperature (columns) and six climate phenomena (rows, right y-axis). Areas of high common spectral density that are above the 95% confidence interval are outlined in black.

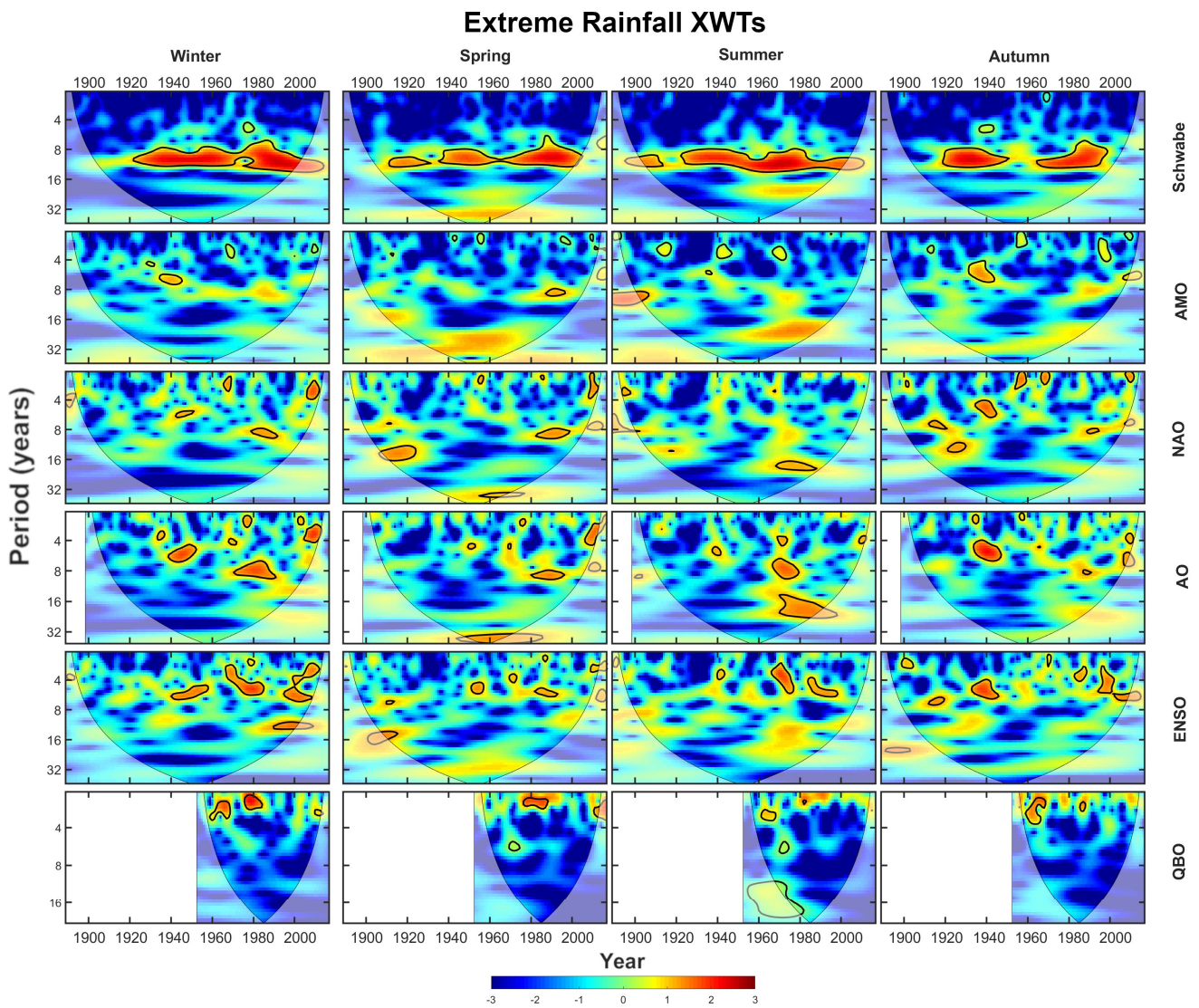


Figure 19. Cross wavelet (XWT) analysis between Ottawa extreme rainfall (columns) and six climate phenomena (rows, right y -axis). Areas of high common spectral density that are above the 95% confidence interval are outlined in black.

Extreme Snowfall XWTs

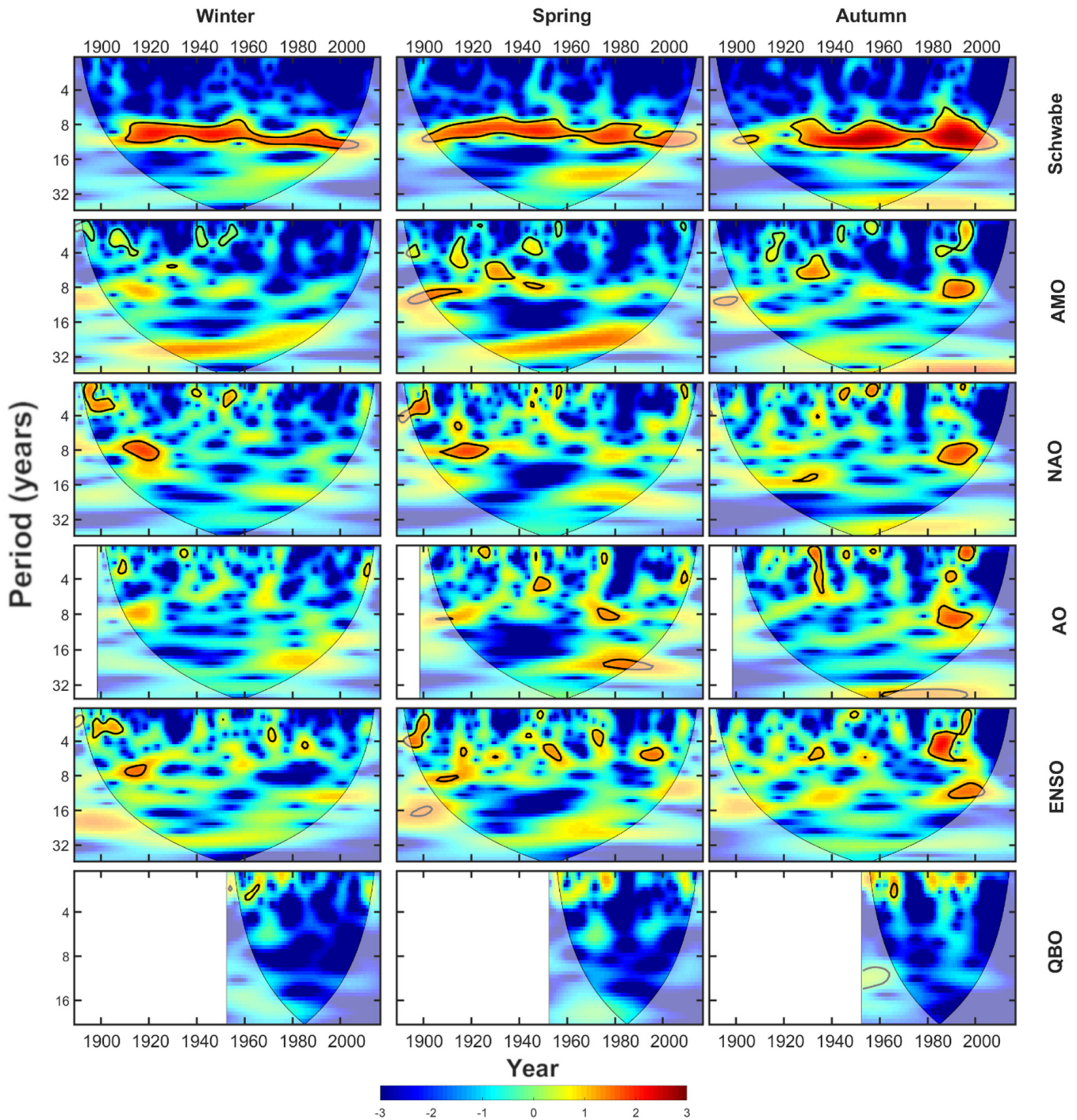


Figure 20. Cross wavelet (XWT) analysis between Ottawa extreme snowfall (columns) and six climate phenomena (rows, right y-axis). Areas of high common spectral density that are above the 95% confidence interval are outlined in black.

5. Discussion

5.1. A Warmer, Wetter Climate

Over the past 130 years, Ottawa’s climate has seen a gradual shift to warmer temperatures, less snow, and more rain. More specifically, there has been an increase in average annual and seasonal maximum and minimum temperature, an increase in annual and seasonal total rainfall, a decrease in annual and seasonal total snowfall, an increase in the

length of the growing season, and an increase in the number of frost-free days. Spring and summer maximum temperatures have remained largely unchanged since 1890, with the exception of year-to-year variations, though daily low temperatures during Ottawa summers have increased and are on par with conditions observed during the other seasons. As previously reported by [15], the most significant long-term changes in Ottawa's climate have predominantly occurred during winter, which has seen a significant increase in maximum and minimum temperatures and rainfall, as well as a large decrease in snowfall. The spring and autumn seasons have generally been characterized by somewhat more moderate changes than during winter, though on a smaller scale, they largely reflect the annual changes that have occurred in Ottawa's climate.

A shift to warmer annual temperatures is consistent with trends reported globally and regionally [91–96]. For Canada in the 20th century, both minimum and maximum temperature trends were near-universally positive during this timeframe (minimum temperatures had a more substantial and significant increase), particularly for southern Canada [4,6,78,97]. In eastern Ontario, the region where Ottawa is located, increases in temperature have been reported at various weather stations in southern Ontario and Quebec [98]. Ref. [99] also noted increases in southern Ontario temperature by as much as 0.1 °C/year from 2001 to 2014, depending on the season and location.

The increase in rainfall and the associated decrease in snowfall in Ottawa is attributable to the general increase in regional temperature, which has turned what formerly would have been snow events into rain events. This transition is consistent with the observed increase in the number of frost-free days and concomitant increase in the length of the growing season. There has also been an overall increase in precipitation over the past 130 years that can be directly attributed to warmer temperatures, as there is a higher rate of evaporation and warmer air has a greater capacity for increased humidity [100]. Similar precipitation trends have been reported from across North America [101,102], and in Canada, a similar decrease in snowfall accompanied by an increase in rainfall has also been observed regionally in southern Ontario and Quebec [78,103,104], as well as in other regions across the country [4,105]. As a consequence of the increased precipitation patterns, the discharge through rivers traversing within the Ottawa area has also increased. This combination of a long-term increase in precipitation overprinted by several cyclical drivers of precipitation with subdecadal to decadal return times (e.g., SSC, ENSO, NAO, AO, QBO) may result in more frequent major flood events in the future. Two particularly significant floods of the Ottawa River took place during spring freshet in 2017 and 2019, which were generally attributed to heavy spring rain and thick winter snowpacks [106]. It is critical that city planners charged with developing Ottawa's New Official Plan fully understand the changing flood risk associated with precipitation that will only continue to grow during the 21st century [107,108].

A further significant long-term trend in Ottawa's climate has been the pronounced decrease in DTR, where there has been a greater increase in minimum temperature than in maximum temperature. In other words, while daytime highs are somewhat warmer now than 130 years ago, the nighttime lows are much warmer than in the past. These changes in DTR are seasonally dependent, being most pronounced during the summer months, with the summer DTR trend being most influential on an average annual DTR trend. A possible explanation for the observed DTR trend is UHIE, which was found to be most significant during summer in Ottawa. As insolation is highest during the summer, Ottawa's urban area, with its considerable number of densely packed buildings, large expanses of pavement, and an associated loss of naturally cooling vegetated landscapes, absorbs a greater amount of heat in the summer compared to other seasons. The increase in these heat-absorbing surfaces means that summer nights have less potential to cool off compared to the other seasons when the sun is tracking lower during the day. The Ottawa-Gatineau Metro area population had increased from just over 100,000 at the end of the 19th century to 282,000 in 1950, was 1.4 million in 2020, and is projected to grow to up to 1.6 million by 2045 [109].

With this considerable population growth, UHIE and associated DTR is an issue that policymakers and planners will need to pay close attention to [28]. A similar trend in decreased DTR was reported by [100] and [4] from many locations across Canada and worldwide [110–112]. Furthermore, ref. [100] found a relationship between decreasing DTR and increases in monthly precipitation. From the results of our study, it is unclear if the decrease in the diurnal temperature range in Ottawa shares a causal relationship with the increase in precipitation. Properly assessing this relationship provides scope for future work.

In addition to the long-term trends in average temperatures in Ottawa described above, there are several significant observable extreme weather trends observable within the instrumental record for this city, specifically:

1. A decrease in extreme minimum temperature events across all seasons.
2. An increase in extreme maximum temperature events in the winter.
3. A decrease of extreme maximum temperature events in the summer.
4. A decrease in extreme snowfall events in the winter.

These four extreme weather trends can somewhat be corroborated against the patterns in annual and seasonal weather discussed previously. An explanation for the decrease in extreme minimum temperature events across the seasons combined with a decrease in extreme maximum and minimum temperature events in the summer follows from the overall observed increases in annual and seasonal temperature through the interval spanned by the instrumental record. This is because the warmer air masses in the mid-latitudes of eastern North America that tend to hold more humidity and which moderates climate are more prevalent today than in earlier decades [113]. As the capacity for the air masses over Ottawa to store humidity has increased, heat is better retained by these air masses, which leads to warmer nights and fewer extreme cold events in the winter or summer. The prior-mentioned significant decrease in DTR in Ottawa is a related phenomenon. At the same time, humid air masses require more energy input to heat up, which may explain the decreased observed frequency of extreme maximum temperature events. In contrast to summer, extreme maximum temperature events in the winter have increased with time. This difference can, once again, be explained by a higher incidence of humid air masses reaching Ottawa [114], which is consistent with observing fewer extreme minimum temperature events in the winter, and fewer extreme minimum and maximum temperature events in the summer. Finally, a decrease in extreme snowfall events in the winter is consistent with the overall temperature rise in Ottawa. A corresponding increase in extreme winter rainfall events might not become established for at least two reasons: (1) most winter precipitation in Ottawa falls in the form of snow, and (2) the incidence of mixed precipitation that falls in the Ottawa Valley in winter. In the latter case, a winter storm that might in the past have been an extreme snowfall event may in more recent times be characterized as a mixture of snow and rain, where neither snow nor rain totals can be characterized as extreme. These results are broadly similar to those patterns previously reported in the literature for the region [5,6,9,11,17,78,79,115,116], although the considerable variety in methodology limits the usefulness of directly comparing these previous studies with our results.

Comparisons of Ottawa's warming trends to those of the smaller or non-urbanized nearby communities of Belleville, Morrisburg, and Chelsea yielded inconclusive results. While there was some indication of statistically different rates of change for Ottawa's minimum and maximum temperatures when compared to these communities, most of the comparisons reflected small or insignificant differences in rates of change. Thus, no statistically significant urban heat island effect could be specifically established for Ottawa. There have been previous claims in the literature that UHIE has contributed to the climate trends in Ottawa as the city's urban footprint has expanded (e.g., [15,16]). However, our comparative results are not sufficient to support this claim. It is notable, though, that the weather station data used for Ottawa was collected at the city's very large 4-sq-km Central Experimental Farm, a location that, while within city limits, does not have the

same environmental characteristics that a centralized urban area would have, but rather that of a vast urban park. The location that Ottawa's weather data has been collected is likely to contribute to the indetermination of our results, as could the location of the other weather stations used here. For example, the communities of Belleville and Morrisburg are both proximal to and climatically moderated by the St. Lawrence Seaway, whereas the Chelsea weather station is located at a higher altitude than Ottawa. Furthermore, ref. [117] generated a heatmap of Ottawa using satellite imagery; this map clearly demonstrates that urbanized areas in Ottawa are hotter than rural areas. However, the location of the Central Experimental Farm weather station can be up to 10 °C cooler than surrounding urban areas [117]; thus, locations of the four weather stations here likely impact the detectability of the UHIE in Ottawa from temperature records alone.

5.2. Periodic Trends Highly Influenced by Regional Climate Cycles

As periodicity in climate records has been regularly observed at global to local scales from millennial to interannual levels [15,118–121], the observed presence of cyclicity in Ottawa's instrumental weather record is to be expected. The strongest observed cyclical influence on Ottawa weather present across all measured weather variables at annual and seasonal scales, as well as for temperature and precipitation extreme events, is the 9–13-year SSC. Refs. [122] and [123] also attributed the occurrence of observed 10–11 years cycles in eastern North American precipitation and temperature records to the SSC. Several other relations between the SSC and extreme temperature and precipitation records have been made regionally around the world, including North America and western Europe [5,6,124–131].

The influence of the AMO on Ottawa seasonal and extreme weather is much weaker than the SSC, although the 16–24-year subharmonic of the AMO [42,62] correlates with many aspects of annual weather in Ottawa, as well as seasonal snowfall (Figures 10, 11 and 16). However, most seasonal and extreme weather records did not indicate a strong relationship with this oscillation, despite the AMO having been demonstrated to strongly affect drought and hydrologic conditions in eastern Canada and the United States, particularly when interacting with other oscillations such as the Pacific Decadal Oscillation [103,132,133]. The absence of AMO–extreme weather and seasonal weather connections in Ottawa may be explained by a more moderate long-term effect of the AMO's 50–90-year band on the inland continental climate of Ottawa, which cannot be detected using XWTs over the ~130-year timeframe available.

Although the direct impact of the AMO on Ottawa's climate record is muted, it has been observed to amplify, reduce, or modulate various other climate phenomena (e.g., NAO, AO, ENSO; [134–136]). This may provide an explanation for the abrupt changes in XWTs between several weather records and AMO, NAO, AO, and ENSO (e.g., extreme maximum and minimum temperature, Figures 17 and 18). The AMO was in its positive phase from approximately 1925–1965 [86]. This period corresponded with the same time interval when extreme maximum temperature was least correlated with NAO, AO, and ENSO, suggesting that the impact of these three phenomena were reduced during the positive phase of AMO and amplified during negative phases. Ref. [136] hypothesized an additional interdependency of these oscillations, determining that the relationship between NAO and ENSO is dependent on the phase of the AMO, where NAO is strengthened when the ENSO and AMO share the same phase (positive or negative). This effect may contribute to the similarity in the relationships observed between NAO and ENSO with extreme seasonal and annual weather variables. An analogous AO–ENSO correlation was described by [137] possibly explaining the pattern observed in the Ottawa record.

Three climate patterns, NAO, AO and ENSO, are often cited as the most prominent influences on regional climate variation and have been observed throughout eastern Canada and the US [7,8,10,26,79,104,119,133,138–140]. For Ottawa, the strongest climatic correlations involving NAO, AO and ENSO are with extreme temperatures, implying that these phenomena are slightly more likely to cause isolated temperature events than average

climate conditions. However, these three oscillations pose a strong influence on average climate conditions during particular phase combinations of the NAO, AO, and ENSO. When the NAO and AO are in their positive phases, and the ENSO is in its negative phase (El Niño), increases in both maximum and minimum temperatures (annual and seasonal) are more likely. When these three oscillations are all positive, Ottawa experiences increases in both rain and snow.

In general, QBO also showed a strong relationship with seasonal and extreme weather variables than with the annual variables, particularly maximum and minimum temperatures, rain, and snow. Few correlations between QBO and weather patterns have previously been made in Canada. Ref. [133] noted an increase of warm winter temperature extremes in the southern Canadian Prairies during the westerly phase of the QBO, though they did not find this same association anywhere in eastern Canada. Similarly, ref. [62] have attributed quasi-biennial oscillations in ice breakup dates in the Maritimes and parts of New England to QBO forcing. Documented links between QBO and extreme precipitation in North America are similarly scarce, though extreme precipitation patterns in Greece and China have been observed to conform to various quasi-biennial oscillations [141–143]. Ref. [144] also linked global precipitation patterns directly to the QBO.

A significant quasi-decadal to interdecadal cycle was also seen in several of the QBO XWTs (e.g., Figure 17), typically occurring between the 1950s and early 1980s. This QBO correlation has previously been interpreted as a modulation by the SSC, typically occurring within 1950–1980, and elsewhere in eastern North America [145–147].

6. Conclusions

Ottawa's climate has evolved considerably through the past 130 years. Annual and seasonal maximum and minimum temperatures have risen, precipitation has shifted to a less snowy, rainier regime, and there have been marked decreases in DTR in daily temperature and increases in the length of the growing season and frost-free days. River discharge has also increased dramatically as a response to the changes shown in precipitation, with a moderate correlation between the local precipitation record and the discharge records of both the Rideau and Ottawa rivers. Many of these shifts, particularly the changes in temperatures, occurred between 1950 and 1980. Steady increases in maximum and minimum temperature were notable during this window, and the DTR stabilized around 1980. Precipitation changes here generally more gradual throughout this 130-year timeframe.

In addition to linear changes, several periodic components were found in Ottawa's instrumental climate record, with a variety of cycles typically ranging between 2–15 years observed. These cycles are attributed to several natural climate oscillations; the strongest of these relationships being the SSC, which strongly and nearly equally influenced the occurrence of quasi-decadal patterns in annual, seasonal, and extreme weather records. The NAO, AO, and ENSO were found to have a stronger relationship with extreme maximum and minimum temperature than over annual or seasonal weather records, potentially indicating a greater likelihood of temperature extremes during stronger phases of these climate oscillations. However, particularly phase combinations of these oscillations, namely NAO+/AO+/ENSO- and NAO+/AO+/ENSO+, were found to increase the likelihood of warmer or wetter years, respectively. These three oscillations were also suspected to be exhibiting some amplification/reduction effects derived from the influence of AMO. On its own, the AMO demonstrated less statistically significant (but still notable) influence by its higher frequency subharmonics, primarily on extreme temperatures, rainfall and snowfall. The influence of QBO accounted for quasi-biennial oscillations in Ottawa's seasonal and extreme weather records. The results of this study will be of utility to City of Ottawa policymakers and planners, as related to infrastructure requirements to accommodate planned intensification as its population rapidly grows under increasingly warmer and wetter climate conditions.

Supplementary Materials: The following supporting information can be downloaded at: <http://www.mdpi.com/article/10.3390/environments9030035/s1>, Figure S1: Smoothed (LOWESS, span|0.15 ± 95%) bar graphs for the seasonal count of extreme weather events in Ottawa, ON; Figure S2: Spectral analysis of annual weather records with indicated red noise (AR1) and significance lines for Ottawa, ON; Figure S3: Continuous wavelet transforms (CWTs) of annual weather records for Ottawa, ON. Areas of high spectral density that are greater than the 90% confidence level are outlined in black; Figure S4: Spectral analysis of seasonal weather records with indicated red noise (AR1) and significance lines for Ottawa, ON; Figure S5: Continuous wavelet transforms (CWTs) of seasonal weather records for Ottawa, ON. Areas of high spectral density that are greater than the 90% confidence level are outlined in black; Figure S6: Spectral analysis of seasonal extreme weather records with indicated red noise (AR1) and significance lines for Ottawa, ON; Figure S7: Continuous wavelet transforms (CWTs) of seasonal extreme weather records for Ottawa, ON. Areas of high spectral density that are greater than the 90% confidence level are outlined in black; Table S1: Changes in various LOWESS-smoothed weather records, 1890–2019; Table S2: Slopes for seasonal temperature comparisons (ΔT) between Ottawa, ON, and each of Belleville, ON, Morrisburg, ON, and Chelsea, QC maximum and minimum temperature time series.

Author Contributions: Conceptualization, C.R.W. and R.T.P.; methodology, C.R.W. and R.T.P.; software, C.R.W.; validation, C.R.W.; formal analysis, C.R.W.; investigation, C.R.W.; resources, C.R.W.; data curation, C.R.W.; writing—original draft preparation, C.R.W.; writing—review and editing, C.R.W. and R.T.P.; visualization, C.R.W. and R.T.P.; supervision, R.T.P.; project administration, C.R.W. and R.T.P.; funding acquisition, R.T.P. All authors have read and agreed to the published version of the manuscript.

Funding: This research was funded by a Natural Sciences and Engineering Research Council of Canada Discovery Grant (RGPIN-2018-05329) to RTP.

Data Availability Statement: The data presented in this study are openly available from Environment and Climate Change Canada [64], the National Oceanic and Atmospheric Association [86–90] and the Royal Observatory of Belgium [85].

Acknowledgments: We thank the Natural Sciences and Engineering Research Council of Canada for funding this research.

Conflicts of Interest: The authors declare no conflict of interest.

Abbreviations

The following abbreviations are used in this manuscript:

SSC	Schwabe Solar Cycle
AMO	Atlantic Multidecadal Oscillation
NAO	North Atlantic Oscillation
AO	Arctic Oscillation
ENSO El	Niño Southern Oscillation
QBO	Quasi-Biennial Oscillation
DTR	Diurnal temperature range
UHIE	Urban heat island effect

References

1. Fitzgerald, J. The Intergovernmental Panel on Climate Change: Taking the first steps towards a global response. *South. Ill. Univ. Law J.* **1989**, *14*, 231.
2. Smith, H.A. Political parties and Canadian climate change policy. *Int. J.* **2009**, *64*, 47–66. [[CrossRef](#)]
3. Boyd, B. Working together on climate change: Policy transfer and convergence in four Canadian provinces. *Publius J. Fed.* **2017**, *47*, 546–571. [[CrossRef](#)]
4. Zhang, X.; Vincent, L.A.; Hogg, W.; Niitsoo, A. Temperature and precipitation trends in Canada during the 20th century. *Atmos. Ocean.* **2000**, *38*, 395–429. [[CrossRef](#)]
5. Zhang, X.; Hogg, W.; Mekis, É. Spatial and temporal characteristics of heavy precipitation events over Canada. *J. Clim.* **2001**, *14*, 1923–1936. [[CrossRef](#)]
6. Bonsal, B.; Zhang, X.; Vincent, L.; Hogg, W. Characteristics of daily and extreme temperatures over Canada. *J. Clim.* **2001**, *14*, 1959–1976. [[CrossRef](#)]

7. Bonsal, B.R.; Prowse, T.D.; Duguay, C.R.; Lacroix, M.P. Impacts of large-scale teleconnections on freshwater-ice break/freeze-up dates over Canada. *J. Hydrol.* **2006**, *330*, 340–353. [CrossRef]
8. Coulibaly, P. Spatial and temporal variability of Canadian seasonal precipitation (1900–2000). *Adv. Water Resour.* **2006**, *29*, 1846–1865. [CrossRef]
9. Shephard, M.W.; Mekis, E.; Morris, R.J.; Feng, Y.; Zhang, X.; Kilcup, K.; Fleetwood, R. Trends in Canadian short-duration extreme rainfall: Including an intensity–duration–frequency perspective. *Atmos. Ocean.* **2014**, *52*, 398–417. [CrossRef]
10. Ning, L.; Bradley, R.S. Winter climate extremes over the northeastern United States and southeastern Canada and teleconnections with large-scale modes of climate variability. *J. Clim.* **2015**, *28*, 2475–2493. [CrossRef]
11. Vincent, L.; Zhang, X.; Mekis, É.; Wan, H.; Bush, E. Changes in Canada’s climate: Trends in indices based on daily temperature and precipitation data. *Atmos. Ocean.* **2018**, *56*, 332–349. [CrossRef]
12. Christensen, J.H.; Kanikicharla, K.K.; Aldrian, E.; An, S.I.; Cavalcanti, I.F.A.; de Castro, M.; Dong, W.; Goswami, P.; Hall, A.; Kanyanga, J.K.; et al. Climate phenomena and their relevance for future regional climate change. In *Climate Change 2013 the Physical Science Basis: Working Group I Contribution to the Fifth Assessment Report of the Intergovernmental Panel on Climate Change*; Cambridge University Press: Cambridge, UK, 2013; pp. 1217–1308.
13. Lennard, C.; Nikulin, G.; Dosio, A.; Moufouma-Okia, W. On the need for regional climate information over Africa under varying levels of global warming. *Environ. Res. Lett.* **2018**, *13*, 060401. [CrossRef]
14. Bootsma, A. Long term (100 yr) climatic trends for agriculture at selected locations in Canada. *Clim. Change* **1994**, *26*, 65–88. [CrossRef]
15. Prokoph, A.; Patterson, R.T. Application of wavelet and regression analysis in assessing temporal and geographic climate variability: Eastern Ontario, Canada as a case study. *Atmos. Ocean.* **2004**, *42*, 201–212. [CrossRef]
16. Adamowski, J.; Prokoph, A. Assessing the impacts of the urban heat island effect on streamflow patterns in Ottawa, Canada. *J. Hydrol.* **2013**, *496*, 225–237. [CrossRef]
17. Ahmed, S.I.; Rudra, R.; Dickinson, T.; Ahmed, M. Trend and periodicity of temperature time series in Ontario. *Am. J. Clim. Change* **2014**, *3*, 272. [CrossRef]
18. Catling, P.M. Climate Warming as an Explanation for the Recent Northward Range Extension of Two Dragonflies, *Pachydiplax longipennis* and *Perithemis tenera*, into the Ottawa Valley, Eastern Ontario. *Can. Field Nat.* **2016**, *130*, 122–132. [CrossRef]
19. Spears, T. An Inconvenient Ottawa? What Will Climate Change Actually Mean for the Nation’s Capital? 2017. Available online: <https://ottawacitizen.com/news/local-news/an-inconvenient-ottawa-what-will-climate-change-actually-mean-for-the-nations-capital> (accessed on 25 February 2022).
20. Osman, L. Ottawa’s Wild Weather ‘The Tip of the Iceberg’, Some Experts Say | CBC News. 2019. Available online: <https://www.cbc.ca/news/canada/ottawa/tornado-climatologist-june-3-1.5159862> (accessed on 25 February 2022).
21. City of Ottawa. Climate Change Master Plan. Technical Report, A Report by Ottawa’s Planning, Development, and Construction Division. 2020. Available online: https://documents.ottawa.ca/sites/documents/files/climate_change_mplan_en.pdf (accessed on 25 February 2022).
22. Kwon, H.H.; Lall, U.; Moon, Y.I.; Khalil, A.F.; Ahn, H. Episodic interannual climate oscillations and their influence on seasonal rainfall in the Everglades National Park. *Water Resour. Res.* **2006**, *42*. [CrossRef]
23. Ogurtsov, M.G.; Raspopov, O.M.; Helama, S.; Oinonen, M.; Lindholm, M.; Jungner, H.; Meriläinen, J. Climatic variability along a north–south transect of Finland over the last 500 years: Signature of solar influence or internal climate oscillations? *Geogr. Ann. Ser. A Phys. Geogr.* **2008**, *90*, 141–150. [CrossRef]
24. Bonsal, B.; Shabbar, A. *Large-Scale Climate Oscillations Influencing Canada, 1900–2008*; Canadian Councils of Resource Ministers: Montreal, QC, Canada, 2011.
25. Chandran, A.; Basha, G.; Ouarda, T. Influence of climate oscillations on temperature and precipitation over the United Arab Emirates. *Int. J. Climatol.* **2016**, *36*, 225–235. [CrossRef]
26. Thiombiano, A.N.; El Adlouni, S.; St-Hilaire, A.; Ouarda, T.B.; El-Jabi, N. Nonstationary frequency analysis of extreme daily precipitation amounts in Southeastern Canada using a peaks-over-threshold approach. *Theor. Appl. Climatol.* **2017**, *129*, 413–426. [CrossRef]
27. Yang, Y.; Gan, T.Y.; Tan, X. Spatiotemporal changes in precipitation extremes over Canada and their teleconnections to large-scale climate patterns. *J. Hydrometeorol.* **2019**, *20*, 275–296. [CrossRef]
28. Lassen, K.; Friis-Christensen, E. Variability of the solar cycle length during the past five centuries and the apparent association with terrestrial climate. *J. Atmos. Terr. Phys.* **1995**, *57*, 835–845. [CrossRef]
29. Rind, D.; Lean, J.; Lerner, J.; Lonergan, P.; Leboissitier, A. Exploring the stratospheric/tropospheric response to solar forcing. *J. Geophys. Res. Atmos.* **2008**, *113*. [CrossRef]
30. Lockwood, M. Solar influence on global and regional climates. *Surv. Geophys.* **2012**, *33*, 503–534. [CrossRef]
31. Hathaway, D.H. The Solar Cycle. *Living Rev. Sol. Phys.* **2015**, *12*, 4. [CrossRef]
32. Schlesinger, M.E.; Ramankutty, N. An oscillation in the global climate system of period 65–70 years. *Nature* **1994**, *367*, 723–726. [CrossRef]
33. Enfield, D.B.; Mestas-Nuñez, A.M.; Trimble, P.J. The Atlantic multidecadal oscillation and its relation to rainfall and river flows in the continental US. *Geophys. Res. Lett.* **2001**, *28*, 2077–2080. [CrossRef]

34. Knight, J.R.; Folland, C.K.; Scaife, A.A. Climate impacts of the Atlantic multidecadal oscillation. *Geophys. Res. Lett.* **2006**, *33*. [[CrossRef](#)]
35. Dima, M.; Lohmann, G. A hemispheric mechanism for the Atlantic Multidecadal Oscillation. *J. Clim.* **2007**, *20*, 2706–2719. [[CrossRef](#)]
36. Feng, S.; Hu, Q.; Oglesby, R.J. Influence of Atlantic sea surface temperatures on persistent drought in North America. *Clim. Dyn.* **2011**, *37*, 569–586. [[CrossRef](#)]
37. Knudsen, M.F.; Seidenkrantz, M.S.; Jacobsen, B.H.; Kuijpers, A. Tracking the Atlantic Multidecadal Oscillation through the last 8000 years. *Nat. Commun.* **2011**, *2*, 1–8. [[CrossRef](#)] [[PubMed](#)]
38. Ruiz-Barradas, A.; Nigam, S.; Kavvada, A. The Atlantic Multidecadal Oscillation in twentieth century climate simulations: Uneven progress from CMIP3 to CMIP5. *Clim. Dyn.* **2013**, *41*, 3301–3315. [[CrossRef](#)]
39. Alexander, M.A.; Kilbourne, K.H.; Nye, J.A. Climate variability during warm and cold phases of the Atlantic Multidecadal Oscillation (AMO) 1871–2008. *J. Mar. Syst.* **2014**, *133*, 14–26. [[CrossRef](#)]
40. Hurrell, J.W. Decadal trends in the North Atlantic Oscillation: Regional temperatures and precipitation. *Science* **1995**, *269*, 676–679. [[CrossRef](#)]
41. Hurrell, J.W.; Kushnir, Y.; Visbeck, M. The North Atlantic Oscillation. *Science* **2001**, *291*, 603–605. [[CrossRef](#)]
42. Hurrell, J.W.; Kushnir, Y.; Ottersen, G.; Visbeck, M. An overview of the North Atlantic oscillation. *Geophys. Monogr. Am. Geophys. Union* **2003**, *134*, 1–36.
43. Olsen, J.; Anderson, N.J.; Knudsen, M.F. Variability of the North Atlantic Oscillation over the past 5200 years. *Nat. Geosci.* **2012**, *5*, 808–812. [[CrossRef](#)]
44. Deser, C. On the teleconnectivity of the Arctic Oscillation. *Geophys. Res. Lett.* **2000**, *27*, 779–782. [[CrossRef](#)]
45. Ambaum, M.H.; Hoskins, B.J.; Stephenson, D.B. Arctic oscillation or North Atlantic oscillation? *J. Clim.* **2001**, *14*, 3495–3507. [[CrossRef](#)]
46. Rogers, J.; McHugh, M. On the separability of the North Atlantic oscillation and Arctic oscillation. *Clim. Dyn.* **2002**, *19*, 599–608.
47. Li, Z.; Manson, A.H.; Li, Y.; Meek, C. Circulation characteristics of persistent cold spells in central–eastern North America. *J. Meteorol. Res.* **2017**, *31*, 250–260. [[CrossRef](#)]
48. Philander, S.G.H. El Niño southern oscillation phenomena. *Nature* **1983**, *302*, 295. [[CrossRef](#)]
49. Ropelewski, C.F.; Halpert, M.S. North American precipitation and temperature patterns associated with the El Niño/Southern Oscillation (ENSO). *Mon. Weather. Rev.* **1986**, *114*, 2352–2362. [[CrossRef](#)]
50. Philander, S.G. *El Niño, La Niña, and the Southern Oscillation*; Academic Press: Cambridge, MA, USA, 1989.
51. Moy, C.M.; Seltzer, G.O.; Rodbell, D.T.; Anderson, D.M. Variability of El Niño/Southern Oscillation activity at millennial timescales during the Holocene epoch. *Nature* **2002**, *420*, 162. [[CrossRef](#)] [[PubMed](#)]
52. Hu, Q.; Feng, S. AMO-and ENSO-driven summertime circulation and precipitation variations in North America. *J. Clim.* **2012**, *25*, 6477–6495. [[CrossRef](#)]
53. Lindzen, R.S.; Holton, J.R. A theory of the quasi-biennial oscillation. *J. Atmos. Sci.* **1968**, *25*, 1095–1107. [[CrossRef](#)]
54. Dunkerton, T.J. The role of gravity waves in the quasi-biennial oscillation. *J. Geophys. Res. Atmos.* **1997**, *102*, 26053–26076. [[CrossRef](#)]
55. Baldwin, M.; Gray, L.; Dunkerton, T.; Hamilton, K.; Haynes, P.; Randel, W.; Holton, J.; Alexander, M.; Hirota, I.; Horinouchi, T.; et al. The quasi-biennial oscillation. *Rev. Geophys.* **2001**, *39*, 179–229. [[CrossRef](#)]
56. Chattopadhyay, J.; Bhatla, R. Possible influence of QBO on teleconnections relating Indian summer monsoon rainfall and sea-surface temperature anomalies across the equatorial pacific. *Int. J. Climatol. A J. R. Meteorol. Soc.* **2002**, *22*, 121–127. [[CrossRef](#)]
57. Sharma, S.; Magnuson, J.J. Oscillatory dynamics do not mask linear trends in the timing of ice breakup for Northern Hemisphere lakes from 1855 to 2004. *Clim. Change* **2014**, *124*, 835–847. [[CrossRef](#)]
58. Patterson, R.T.; Swindles, G.T. Influence of ocean–atmospheric oscillations on lake ice phenology in eastern North America. *Clim. Dyn.* **2015**, *45*, 2293–2308. [[CrossRef](#)]
59. Gray, L.J.; Anstey, J.A.; Kawatani, Y.; Lu, H.; Osprey, S.; Schenzinger, V. Surface impacts of the quasi biennial oscillation. *Atmos. Chem. Phys.* **2018**, *18*, 8227–8247. [[CrossRef](#)]
60. United Nations. *Climate Trends and Variations Bulletin for Canada*; Government of Canada: Ottawa, ON, Canada, 1998.
61. Oke, T.R.; Maxwell, G.B. Urban heat island dynamics in Montreal and Vancouver. *Atmos. Environ.* **1975**, *9*, 191–200. [[CrossRef](#)]
62. Akbari, H.; Konopacki, S. Energy effects of heat-island reduction strategies in Toronto, Canada. *Energy* **2004**, *29*, 191–210. [[CrossRef](#)]
63. Touchaei, A.; Wang, Y. Characterizing urban heat island in Montreal (Canada)—Effect of urban morphology. *Sustain. Cities Soc.* **2015**, *19*, 395–402. [[CrossRef](#)]
64. Environment and Climate Change Canada. Historical Data. Available online: https://climate.weather.gc.ca/historical_data/search_historic_data_e.html (accessed on 20 January 2020).
65. Cleveland, W.S. Robust locally weighted regression and smoothing scatterplots. *J. Am. Stat. Assoc.* **1979**, *74*, 829–836. [[CrossRef](#)]
66. Cleveland, W.S. LOWESS: A program for smoothing scatterplots by robust locally weighted regression. *Am. Stat.* **1981**, *35*, 54. [[CrossRef](#)]

67. Statistics Canada. Census Profile, 2016 Census Chelsea, Municipalité [Census Subdivision], Quebec [Province]. Available online: <https://www12.statcan.gc.ca/census-recensement/2016/dp-pd/prof/details/page.cfm?Lang=E&Geo1=CSD&Code1=2482025&Geo2=PR&Code2=24&Data=Count&SearchType=Begins&SearchPR=01&B1=All> (accessed on 11 November 2020).
68. Statistics Canada. Census Profile, 2016 Census Belleville [Population Centre], Ontario [Province]. Available online: <http://www12.statcan.ca/census-recensement/2011/dp-pd/prof/details/page.cfm?Lang=E&Geo1=CMA&Code1=522&Geo2=PR&Code2=35&Data=Count&SearchText=Belleville&SearchType=Begins&SearchPR=01&B1=All&Custom=&TABID=1> (accessed on 11 November 2020).
69. Statistics Canada. Census Profile, 2016 Census Morrisburg [Population centre], Ontario [Province]. Available online: <https://www12.statcan.gc.ca/census-recensement/2016/dp-pd/prof/details/page.cfm?Lang=E&Geo1=POPC&Code1=0556&Geo2=PR&Code2=35&SearchText=Morrisburg&SearchType=Begins&SearchPR=01&B1=All&GeoLevel=PR&GeoCode=0556&TABID=1&type=0> (accessed on 11 November 2020).
70. Environment Canada. *World Population Prospects 2019, Online Edition. Rev. 1*; Department of Economic and Social Affairs, Population Division, United Nations: New York, NY, USA, 2019.
71. Andrade, J.; Estévez-Pérez, M. Statistical comparison of the slopes of two regression lines: A tutorial. *Anal. Chim. Acta* **2014**, *838*, 1–12. [[CrossRef](#)]
72. Frich, P.; Alexander, L.V.; Della-Marta, P.; Gleason, B.; Haylock, M.; Tank, A.K.; Peterson, T. Observed coherent changes in climatic extremes during the second half of the twentieth century. *Clim. Res.* **2002**, *19*, 193–212. [[CrossRef](#)]
73. Linderholm, H.W. Growing season changes in the last century. *Agric. For. Meteorol.* **2006**, *137*, 1–14. [[CrossRef](#)]
74. Lin, X.; Harrington, J.; Ciampitti, I.; Gowda, P.; Brown, D.; Kisekka, I. Kansas trends and changes in temperature, precipitation, drought, and frost-free days from the 1890s to 2015. *J. Contemp. Water Res. Educ.* **2017**, *162*, 18–30. [[CrossRef](#)]
75. Government of Canada. *Water Level and Flow*; Government of Canada: Ottawa, ON, Canada, 2020.
76. Rahmstorf, S.; Coumou, D. Increase of extreme events in a warming world. *Proc. Natl. Acad. Sci. USA* **2011**, *108*, 17905–17909. [[CrossRef](#)] [[PubMed](#)]
77. Frei, A.; Kunkel, K.E.; Matonse, A. The seasonal nature of extreme hydrological events in the northeastern United States. *J. Hydrometeorol.* **2015**, *16*, 2065–2085. [[CrossRef](#)]
78. Yagouti, A.; Boulet, G.; Vincent, L.; Vescovi, L.; Mekis, E. Observed changes in daily temperature and precipitation indices for southern Québec, 1960–2005. *Atmos. Ocean.* **2008**, *46*, 243–256. [[CrossRef](#)]
79. Tan, X.; Gan, T.Y. Non-stationary analysis of the frequency and intensity of heavy precipitation over Canada and their relations to large-scale climate patterns. *Clim. Dyn.* **2017**, *48*, 2983–3001. [[CrossRef](#)]
80. Dorothée. Red Noise Confidence Levels. Available online: <https://www.mathworks.com/matlabcentral/fileexchange/45539-red-noise-confidencelevels> (accessed on 11 February 2020).
81. Thomson, D.J. Spectrum estimation and harmonic analysis. *Proc. IEEE* **1982**, *70*, 1055–1096. [[CrossRef](#)]
82. Schulz, M.; Mudelsee, M. REDFIT: Estimating red-noise spectra directly from unevenly spaced paleoclimatic time series. *Comput. Geosci.* **2002**, *28*, 421–426. [[CrossRef](#)]
83. Grinsted, A.; Moore, J.C.; Jevrejeva, S. Application of the cross wavelet transform and wavelet coherence to geophysical time series. *Nonlinear Processes Geophys.* **2004**, *11*, 561–566. [[CrossRef](#)]
84. Crosta, X.; Debret, M.; Denis, D.; Courty, M.; Ther, O. Holocene long- and short-term climate changes off Adélie Land, East Antarctica. *Geochem. Geophys. Geosyst.* **2007**, *8*. [[CrossRef](#)]
85. Sunspot Index and Long Term Solar Observations. Total Sunspot Number. Royal Observatory of Belgium, Brussels, Belgium. Available online: <http://www.sidc.be/silso> (accessed on 25 February 2022).
86. Trenberth, K.; Zhang, R.; National Center for Atmospheric Research Staff. The Climate Data Guide: Atlantic Multi-Decadal Oscillation (AMO). Available online: <https://climatedataguide.ucar.edu/climate-data/atlantic-multi-decadal-oscillation-amo> (accessed on 25 February 2022).
87. Hurrell, J.; National Center for Atmospheric Research Staff. The Climate Data Guide: Hurrell North Atlantic Oscillation. (NAO) Index (Station-Based). Available online: <https://climatedataguide.ucar.edu/climate-data/hurrell-north-atlantic-oscillation-nao-index-station-based> (accessed on 25 February 2022).
88. National Center for Atmospheric Research Staff. The Climate Data Guide: Hurrell Wintertime SLP-Based Northern Annular Mode (NAM) Index. Available online: <https://climatedataguide.ucar.edu/climate-data/hurrell-wintertime-slp-based-northern-annular-mode-nam-index> (accessed on 25 February 2022).
89. Trenberth, K.; National Center for Atmospheric Research Staff. The Climate Data Guide: Nino SST Indices (Nino 1 + 2, 3, 3.4, 4, ONI and TNI). Available online: <https://climatedataguide.ucar.edu/climate-data/nino-sst-indices-nino-12-3-34-4-oni-and-tni> (accessed on 25 February 2022).
90. National Center for Atmospheric Research Staff. The Climate Data Guide: QBO: Quasi-Biennial Oscillation). Available online: <https://climatedataguide.ucar.edu/climate-data/qbo-quasi-biennial-oscillation> (accessed on 25 February 2022).
91. Groisman, P.Y.; Easterling, D.R. Variability and trends of total precipitation and snowfall over the United States and Canada. *J. Clim.* **1994**, *7*, 184–205. [[CrossRef](#)]
92. Karoly, D.J.; Wu, Q. Detection of regional surface temperature trends. *J. Clim.* **2005**, *18*, 4337–4343. [[CrossRef](#)]
93. Millett, B.; Johnson, W.C.; Guntenspergen, G. Climate trends of the North American prairie pothole region 1906–2000. *Clim. Change* **2009**, *93*, 243–267. [[CrossRef](#)]

94. Polley, H.W.; Briske, D.D.; Morgan, J.A.; Wolter, K.; Bailey, D.W.; Brown, J.R. Climate change and North American rangelands: Trends, projections, and implications. *Rangel. Ecol. Manag.* **2013**, *66*, 493–511. [[CrossRef](#)]
95. Hegerl, G.C.; Brönnimann, S.; Schurer, A.; Cowan, T. The early 20th century warming: Anomalies, causes, and consequences. *Wiley Interdiscip. Rev. Clim. Change* **2018**, *9*, e522. [[CrossRef](#)]
96. Biskaborn, B.K.; Smith, S.L.; Noetzli, J.; Matthes, H.; Vieira, G.; Streletskiy, D.A.; Schoeneich, P.; Romanovsky, V.E.; Lewkowicz, A.G.; Abramov, A.; et al. Permafrost is warming at a global scale. *Nat. Commun.* **2019**, *10*, 1–11. [[CrossRef](#)] [[PubMed](#)]
97. Chen, Y.; She, Y. Long-term variations of river ice breakup timing across Canada and its response to climate change. *Cold Reg. Sci. Technol.* **2020**, *176*, 103091. [[CrossRef](#)]
98. Nalley, D.; Adamowski, J.; Khalil, B.; Ozga-Zielinski, B. Trend detection in surface air temperature in Ontario and Quebec, Canada during 1967–2006 using the discrete wavelet transform. *Atmos. Res.* **2013**, *132*, 375–398. [[CrossRef](#)]
99. Murfitt, J.; Brown, L.C. Lake ice and temperature trends for Ontario and Manitoba: 2001 to 2014. *Hydrol. Processes* **2017**, *31*, 3596–3609. [[CrossRef](#)]
100. Karl, T.R.; Kukla, G.; Gavin, J. Relationship between decreased temperature range and precipitation trends in the United States and Canada, 1941–1980. *J. Clim. Appl. Meteorol.* **1986**, *25*, 1878–1886. [[CrossRef](#)]
101. Gan, T.Y. Trends in air temperature and precipitation for Canada and north-eastern USA. *Int. J. Climatol.* **1995**, *15*, 1115–1134. [[CrossRef](#)]
102. Easterling, D.R.; Wallis, T.W.; Lawrimore, J.H.; Heim, R.R., Jr. Effects of temperature and precipitation trends on US drought. *Geophys. Res. Lett.* **2007**, *34*. [[CrossRef](#)]
103. Assani, A.; Landry, R.; Laurencelle, M. Comparison of interannual variability modes and trends of seasonal precipitation and streamflow in southern Quebec (Canada). *River Res. Appl.* **2012**, *28*, 1740–1752. [[CrossRef](#)]
104. Nalley, D.; Adamowski, J.; Khalil, B. Using discrete wavelet transforms to analyze trends in streamflow and precipitation in Quebec and Ontario (1954–2008). *J. Hydrol.* **2012**, *475*, 204–228. [[CrossRef](#)]
105. Mekis, É.; Vincent, L.A. An overview of the second generation adjusted daily precipitation dataset for trend analysis in Canada. *Atmos. Ocean.* **2011**, *49*, 163–177. [[CrossRef](#)]
106. McNeil, D. An Independent Review of the 2019 Flood Events in Ontario. Technical report, A Report to the Hon. John Yakabuski, Ontario Minister of Natural Resources and Forestry. 2019. Available online: <https://files.ontario.ca/mnrf-english-ontario-special-advisor-on-flooding-report-2019-11-25.pdf> (accessed on 25 February 2022).
107. Cunderlik, J.M.; Simonovic, S.P. Hydrological extremes in a southwestern Ontario river basin under future climate conditions/Extrêmes hydrologiques dans un bassin versant du sud-ouest de l’Ontario sous conditions climatiques futures. *Hydrol. Sci. J.* **2005**, *50*. [[CrossRef](#)]
108. Thistlethwaite, J.; Henstra, D. Municipal flood risk sharing in Canada: A policy instrument analysis. *Can. Water Resources. J. Rev. Can. Des Ressources Hydr.* **2017**, *42*, 349–363. [[CrossRef](#)]
109. City Of Ottawa. *Growth Projections for the New Official Plan: Methods and Assumptions for Population, Housing and Employment 2018 to 2046*; Technical Report; City of Ottawa: Ottawa, ON, Canada, 2019.
110. Hansen, J.; Sato, M.; Ruedy, R. Long-term changes of the diurnal temperature cycle: Implications about mechanisms of global climate change. *Atmos. Res.* **1995**, *37*, 175–209. [[CrossRef](#)]
111. Price, C.; Michaelides, S.; Pashiardis, S.; Alpert, P. Long term changes in diurnal temperature range in Cyprus. *Atmos. Res.* **1999**, *51*, 85–98. [[CrossRef](#)]
112. Braganza, K.; Karoly, D.J.; Arblaster, J.M. Diurnal temperature range as an index of global climate change during the twentieth century. *Geophys. Res. Lett.* **2004**, *31*. [[CrossRef](#)]
113. Vanos, J.; Cakmak, S. Changing air mass frequencies in Canada: Potential links and implications for human health. *Int. J. Biometeorol.* **2014**, *58*, 121–135. [[CrossRef](#)]
114. Aguado, E.; Burt, J.E. *Understanding Weather & Climate*, 5th ed.; Pearson Prentice Hall: Upper Saddle River, NJ, USA, 2010.
115. Allen, S.M.; Gough, W.A.; Mohsin, T. Changes in the frequency of extreme temperature records for Toronto, Ontario, Canada. *Theor. Appl. Climatol.* **2015**, *119*, 481–491. [[CrossRef](#)]
116. Soulis, E.; Sarhadi, A.; Tinel, M.; Suthar, M. Extreme precipitation time trends in Ontario, 1960–2010. *Hydrol. Processes* **2016**, *30*, 4090–4100. [[CrossRef](#)]
117. Ottawa Public Health. City of Ottawa Urban Heat Island Map [map]. Technical Report, City of Ottawa. 2019. Available online: <https://www.ottawapublichealth.ca/en/public-health-topics/resources/Documents/Urban-Island-Heat-Map-1-City-Wide---EN.pdf> (accessed on 25 February 2022).
118. Zhao, H.; Higuchi, K.; Waller, J.; Auld, H.; Mote, T. The impacts of the PNA and NAO on annual maximum snowpack over southern Canada during 1979–2009. *Int. J. Climatol.* **2013**, *33*, 388–395. [[CrossRef](#)]
119. Nalley, D.; Adamowski, J.; Khalil, B.; Biswas, A. Inter-annual to inter-decadal streamflow variability in Quebec and Ontario in relation to dominant large-scale climate indices. *J. Hydrol.* **2016**, *536*, 426–446. [[CrossRef](#)]
120. Champagne, O.; Arain, M.A.; Coulibaly, P. Atmospheric circulation amplifies shift of winter streamflow in Southern Ontario. *J. Hydrol.* **2019**, *578*, 124051. [[CrossRef](#)]
121. Champagne, O.; Leduc, M.; Coulibaly, P.; Arain, M.A. Winter hydrometeorological extreme events modulated by large-scale atmospheric circulation in southern Ontario. *Earth Syst. Dyn.* **2020**, *11*, 301–318. [[CrossRef](#)]
122. Vines, R. Rainfall patterns in the eastern United States. *Clim. Change* **1984**, *6*, 79–98. [[CrossRef](#)]

123. Currie, R.G. Luni-solar 18.6-and solar cycle 10–11-year signals in USA air temperature records. *Int. J. Climatol.* **1993**, *13*, 31–50. [[CrossRef](#)]
124. Vines, R. Possible relationships between rainfall, crop yields and the Sunspot cycle. *J. Aust. Inst. Agricultural Sci.* **1977**, *43*, 3–13.
125. Vines, R. Analyses of South African rainfall. *South Afr. J. Sci.* **1980**, *76*, 404–409.
126. Vines, R. Rainfall patterns in India. *J. Climatol.* **1986**, *6*, 135–148. [[CrossRef](#)]
127. Currie, R.G.; O'Brien, D.P. Periodic 18.6-year and cyclic 10 to 11 year signals in northeastern United States precipitation data. *J. Climatol.* **1988**, *8*, 255–281. [[CrossRef](#)]
128. Currie, R.G.; Vines, R.G. Evidence for luni-solar and solar cycle signals in Australian rainfall data. *Int. J. Climatol.* **1996**, *16*, 1243–1265. [[CrossRef](#)]
129. Van Loon, H.; Shea, D.J. A probable signal of the 11-year solar cycle in the troposphere of the Northern Hemisphere. *Geophys. Res. Lett.* **1999**, *26*, 2893–2896. [[CrossRef](#)]
130. Maliniemi, V.; Asikainen, T.; Mursula, K. Spatial distribution of Northern Hemisphere winter temperatures during different phases of the solar cycle. *J. Geophys. Res. Atmos.* **2014**, *119*, 9752–9764. [[CrossRef](#)]
131. Laurenz, L.; Lüdecke, H.J.; Lüning, S. Influence of solar activity changes on European rainfall. *J. Atmos. Sol.-Terr. Phys.* **2019**, *185*, 29–42. [[CrossRef](#)]
132. McCabe, G.J.; Palecki, M.A.; Betancourt, J.L. Pacific and Atlantic Ocean influences on multidecadal drought frequency in the United States. *Proc. Natl. Acad. Sci. USA* **2004**, *101*, 4136–4141. [[CrossRef](#)]
133. Shabbar, A.; Bonsal, B. Associations between low frequency variability modes and winter temperature extremes in Canada. *Atmos. Ocean.* **2004**, *42*, 127–140.
134. Zhang, L.; Wang, C.; Wu, L. Low-frequency modulation of the Atlantic warm pool by the Atlantic Multidecadal Oscillation. *Clim. Dyn.* **2012**, *39*, 1661–1671. [[CrossRef](#)]
135. Kang, I.S.; No, H.h.; Kucharski, F. ENSO amplitude modulation associated with the mean SST changes in the tropical central Pacific induced by Atlantic Multidecadal Oscillation. *J. Clim.* **2014**, *27*, 7911–7920. [[CrossRef](#)]
136. Zhang, W.; Mei, X.; Geng, X.; Turner, A.G.; Jin, F.F. A nonstationary ENSO–NAO relationship due to AMO modulation. *J. Clim.* **2019**, *32*, 33–43. [[CrossRef](#)]
137. Li, F.; Wang, H.; Liu, J. The strengthening relationship between Arctic Oscillation and ENSO after the mid-1990s. *Int. J. Climatol.* **2014**, *34*, 2515–2521. [[CrossRef](#)]
138. Anctil, F.; Coulibaly, P. Wavelet analysis of the interannual variability in southern Québec streamflow. *J. Clim.* **2004**, *17*, 163–173. [[CrossRef](#)]
139. Griffiths, M.L.; Bradley, R.S. Variations of twentieth-century temperature and precipitation extreme indicators in the northeast United States. *J. Clim.* **2007**, *20*, 5401–5417. [[CrossRef](#)]
140. Tan, X.; Gan, T.Y.; Shao, D. Wavelet analysis of precipitation extremes over Canadian ecoregions and teleconnections to large-scale climate anomalies. *J. Geophys. Res. Atmos.* **2016**, *121*, 14–469. [[CrossRef](#)]
141. Nastos, P.; Zerefos, C. On extreme daily precipitation totals at Athens, Greece. *Adv. Geosci.* **2007**, *10*, 59–66. [[CrossRef](#)]
142. Becker, S.; Hartmann, H.; Coulibaly, M.; Zhang, Q.; Jiang, T. Quasi periodicities of extreme precipitation events in the Yangtze River basin, China. *Theor. Appl. Climatol.* **2008**, *94*, 139–152. [[CrossRef](#)]
143. Han, T.; Li, S.; Hao, X.; Guo, X. A statistical prediction model for summer extreme precipitation days over the northern central China. *Int. J. Climatol.* **2020**, *40*, 4189–4202. [[CrossRef](#)]
144. Lau, K.M.; Sheu, P. Annual cycle, Quasi-Biennial Oscillation, and Southern Oscillation in global precipitation. *J. Geophys. Res. Atmos.* **1988**, *93*, 10975–10988. [[CrossRef](#)]
145. Quiroz, R.S. Period modulation of the stratospheric Quasi-Biennial Oscillation. *Mon. Weather. Rev.* **1981**, *109*, 665–674. [[CrossRef](#)]
146. Hamilton, K. On the quasi-decadal modulation of the stratospheric QBO period. *J. Clim.* **2002**, *15*, 2562–2565. [[CrossRef](#)]
147. Fischer, P.; Tung, K. A reexamination of the QBO period modulation by the solar cycle. *J. Geophys. Res. Atmos.* **2008**, *113*. [[CrossRef](#)]